Geophys. J. Int. (1999) **137,** 891–908

Microseismicity and focal mechanisms at the western termination of the North Anatolian Fault and their implications for continental tectonics

Denis Hatzfeld,[1] Maria Ziazia,[2] Despina Kementzetzidou,[1] Panayotis Hatzidimitriou,[3] Dimitris Panagiotopoulos,[3] Kostas Makropoulos,[2] Panayotis Papadimitriou[2] and Anne Deschamps[4]

[1] *Laboratoire de Géophysique Interne et Tectonophysique, IRIGM-CNRS,* BPP53X, 38041 *Grenoble Cedex* 9, *France.*
E-mail: Denis.Hatzfeld@ujf-grenoble.fr
[2] *Department of Geophysics, University of Athens, Ilissia,* 15784 *Athens, Greece*
[3] *Geophysical Laboratory, Aristotle University,* BP 352–01, 54006 *Thessaloniki, Greece*
[4] *Géosciences-Azur,* 250 *av. Albert Einstein,* 06560 *Valbonne, France*

Accepted 1999 January 29. Received 1998 October 10; in original form 1997 December 3

SUMMARY

For seven weeks, a temporary network of 68 seismological stations was operated in Central Greece, in the region of Thessaly and Evia, located at the western termination of the North Anatolian Fault system. We recorded 510 earthquakes and computed 80 focal mechanisms. Seismic activity is associated with the NE–SW dextral North Aegean Fault, or with very young E–W-striking normal faults that are located around the Gulf of Volos and the Gulf of Lamia. The important NW–SE-striking faults bounding the Pilion, or the basins of Larissa and Karditsa, are not seismically active, suggesting that it is easier to break continental crust, creating new faults perpendicular to the principal stresses, than to reactivate faults that strike obliquely to the principal stress axes

Key words: continental deformation, faulting, microearthquakes, seismotectonics.

INTRODUCTION

Continental deformation is commonly more complicated than plate tectonics predicts, for it is not limited to narrow boundaries between rigid lithospheric plates, but affects wide areas with horizontal dimensions much larger than the lithosphere thickness (England & Jackson 1989). The strength of continental lithosphere appears to be less than that of oceanic lithosphere, in part because most continental regions have been affected by previous tectonic events. Crustal blocks move relative to one another generally in a complex kinematic scheme, and the origins of the forces that drive the crustal blocks still remain a matter of debate. To what extent does the upper crust passively respond to the motion of a ductile lower crust and upper mantle (e.g. England & McKenzie 1982; Molnar 1988; Lamb 1994), or to forces applied to its edges (e.g. Tapponnier 1977; Nur *et al.* 1986)?

The Aegean region (Figs 1 and 2) is one of the most rapidly deforming regions in the continental domain (Jackson 1994; Papazachos & Kiratzi 1996). Although located between the two major lithospheric plates of Eurasia and Africa, whose 1 cm yr^{-1} convergent motion is approximately N–S (McKenzie 1972, 1978; De Mets *et al.* 1990), the Hellenic Trench moves southwestwards at about 3.5 cm yr^{-1} with respect to Eurasia and requires extension of approximately that amount within the Aegean (Noomen *et al.* 1995).

The North Aegean region is affected by intense deformation. The seismicity is relatively high and defines a limited number of active features (Fig. 1). The most prominent is the North Aegean Trough, which forms one of the three branches of the western continuation of the North Anatolian Fault (Lyberis 1984; Jackson & McKenzie 1988; Taymaz *et al.* 1991). In contrast, in the southern Aegean (Peloponnese, Sea of Crete, Dodecanese and Cyclades islands), extension of $\sim$1.0–1.5 cm yr^{-1} occurs nearly parallel to the Hellenic Trench (Noomen *et al.* 1995, Robbins *et al.* 1994; Kastens *et al.* 1995).

Several geodynamical models have been proposed to explain the deformation and the kinematics of the North Aegean. Some models imply one (McKenzie 1972) or two (Le Pichon *et al.* 1995) small rigid lithospheric plates that move relative to Eurasia. Others include crustal blocks of smaller size (e.g. McKenzie & Jackson 1983; Taymaz *et al.* 1991) that interact over a viscoplastic substratum (e.g. England *et al.* 1985).

In some models, the geodynamics of the Aegean is governed by the motion of Arabia and Turkey relative to Eurasia, which implies a synchronous motion for both the North Anatolian Fault and the Aegean. However, the extension that affects the Aegean region began a least 15 Myr ago and therefore it is

© 1999 RAS

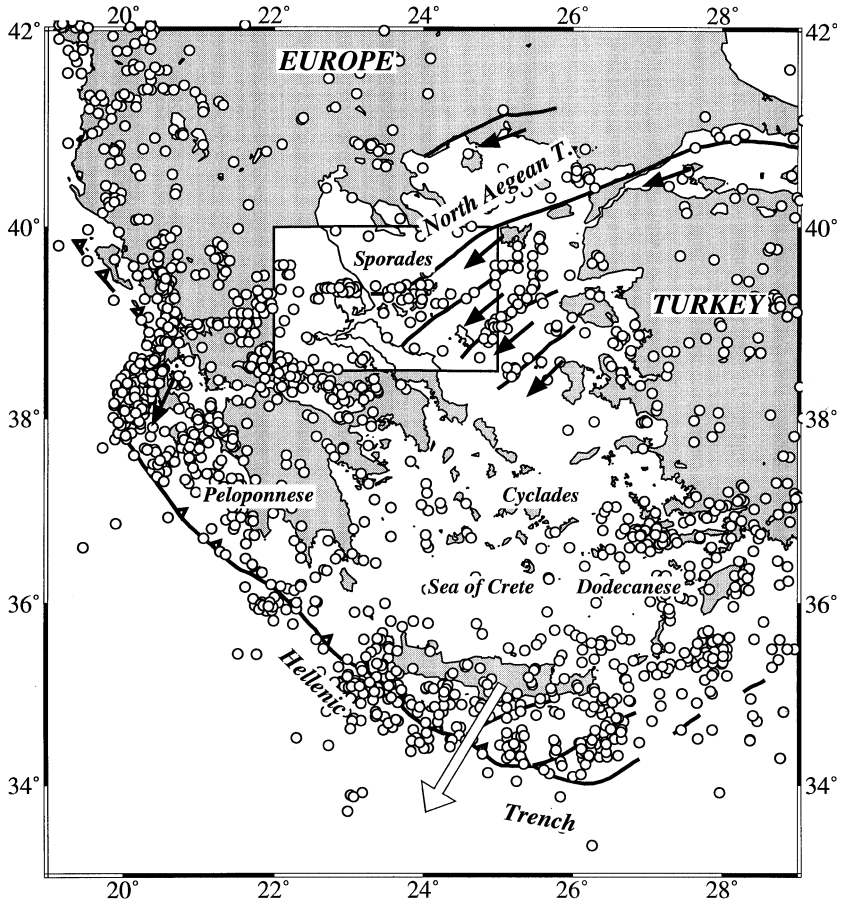

Figure 1. General sketch of the Aegean showing seismicity and geographical names. White dots mark locations of earthquakes of magnitude greater than 4.5 from 1963 to 1996 located by the NEIS. The white arrow shows the motion of Aegea relative to Europe. The box surrounds the area studied here.

earlier than the Upper Miocene start of motion along the North Aegean Trough (Angelier *et al.* 1982; Mercier *et al.* 1989; Jolivet *et al.* 1994). Therefore, the geodynamics of the Aegean seems to be independent of (or only weakly dependent on) the movement of Anatolia (Le Pichon *et al.* 1995). McKenzie & Jackson (1983) proposed that the NE–SW right-lateral strike-slip motion on the North Aegean Trough is taken up on a wide zone of normal faulting that is responsible for block rotations. Pavlides & Caputo (1994) suggested that the North Anatolian Fault propagated southwestwards into the Aegean. Armijo *et al.* (1996) proposed that this fault is deeply rooted in the lithosphere and that its propagation is responsible for the recent increase of tectonic activity in the pre-existing rifts of the North Evia Basin, the Gulf of Evia and the Gulf of Corinth. This increase of activity in the Gulf of Corinth 1 Myr ago is synchronous with a change in direction of the extension that is documented in most of the Northern Aegean region such as the Mygdonia graben (Mercier *et al.* 1983), western Macedonia (Pavlides & Mountrakis 1987) and Thessaly (Caputo & Pavlides 1993).

In this context, we studied the seismotectonics of the western termination of the North Aegean Trough and its relationship with the tectonics of continental Greece in order to address the questions related to the tectonics (active faulting) and kinematics (both in space and in time) of this area and infer its possible dynamics.

SEISMICITY AND TECTONICS

The North Aegean Trough follows the western continuation of the dextral strike-slip North Anatolian Fault, which in western Turkey, before entering the North Aegean Sea, splits into three branches (Taymaz *et al.* 1991). The northern branch is the most seismically active (Figs 1 and 2) and is associated with an important bathymetric feature connected to the Saros and Sporades basins with a depth of 1500 m (Lyberis 1984), which were reactivated during Pliocene time (Dinter & Royden 1993). In contrast, the southern branch is less developed, the associated basins are not as deep, and the amount of motion along the fault zone is probably smaller (Mascle & Martin 1990).

All three branches of the North Aegean Fault stop abruptly at the Saros and Northern Evia basins. No well-defined tectonic structure responsible for the transfer of motion to the Gulf of Evia and the Gulf of Corinth has been recognized. The Saros and Evia basins are bounded, east of Pilion and east of Evia, by very important NW–SE-striking faults that were active during Pliocene time (Caputo 1990; Roberts & Jackson 1991; Armijo *et al.* 1996).

The tectonics of continental Greece underwent changes in late Cenozoic time that varied from region to region. In Thessaly, after the orogenic compressive episode that affected western Greece during the Early Miocene, two different

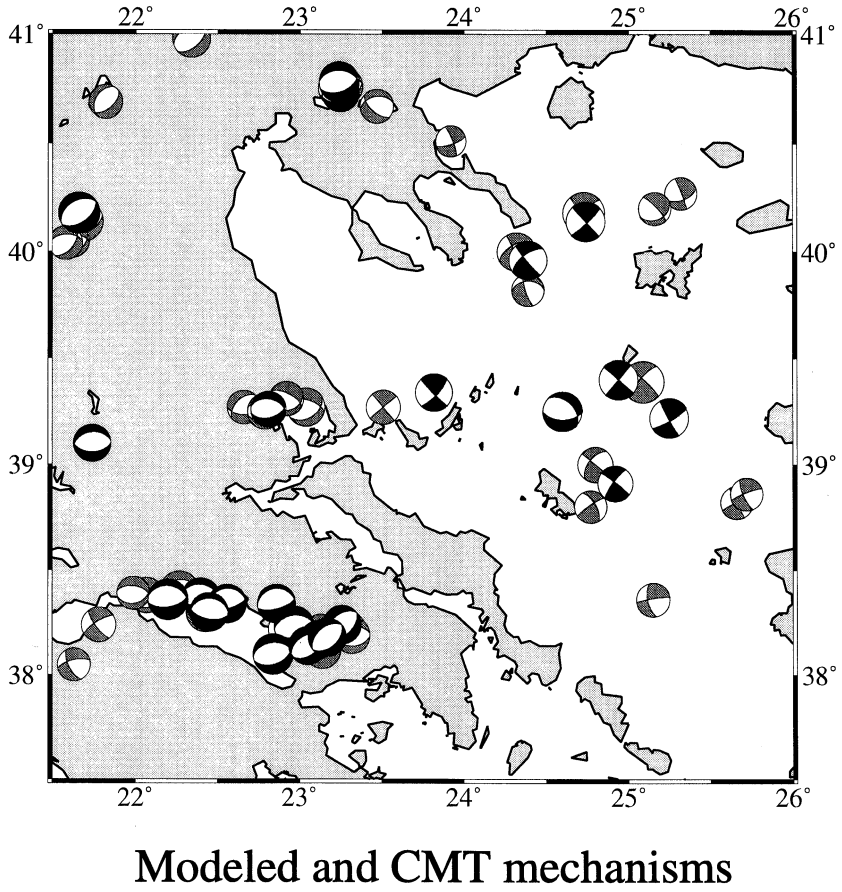

Figure 2. Map showing lower-hemisphere projections of focal mechanisms computed in the northwest Aegean region for teleseismic data. Black and grey quadrants include compressional first motions for mechanisms modelled by Taymaz *et al.* (1991) and Harvard CMT solutions, respectively.

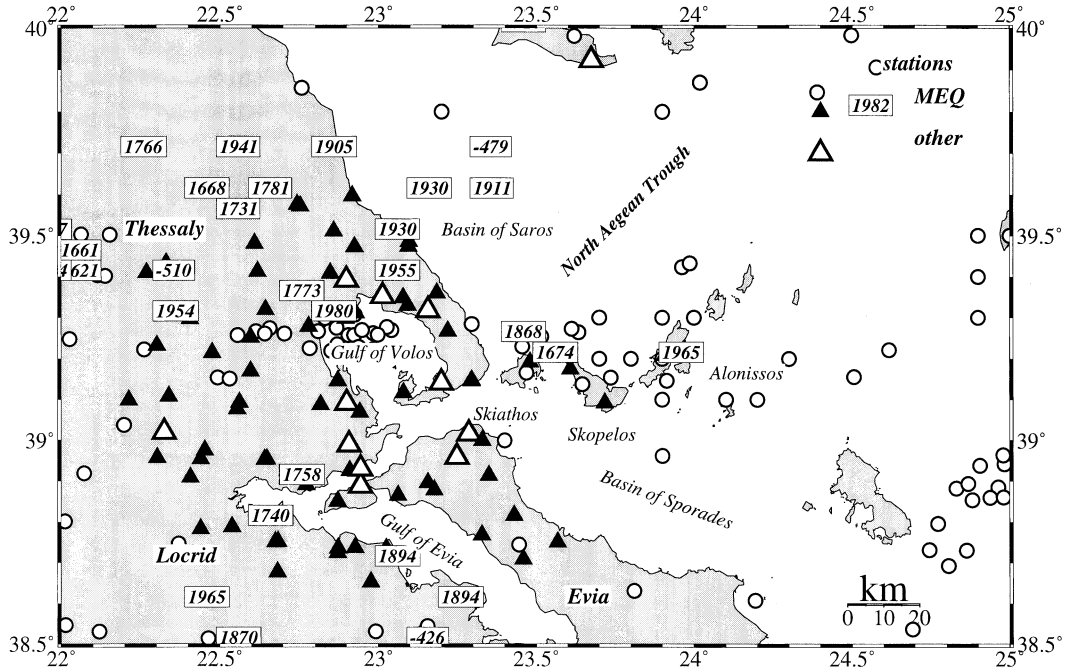

Figure 3. Map of the temporary seismological network installed in Thessaly and Locrid during the summer of 1992 for seven weeks. The locations of historical earthquakes (Papazachos & Papazachou 1997) and of earthquakes with magnitudes greater than 4.5 (NEIS) are shown by boxes and circles, respectively. The smoked paper and digital seismological stations are shown by open and filled triangles, respectively.

extension phases are observed. The first extension phase (Late Miocene–Pliocene), possibly due to post-orogenic collapse, trended NE–SW (Mercier *et al.* 1976, 1979; Caputo & Pavlides 1993) and created the two important basins of Larissa and Karditsa. The second extension phase, trending N–S, started in the Middle Pleistocene and activated many E–W-striking faults. The later episode is certainly the less well developed, with extension of only $\sim 1\,\mathrm{mm\,yr^{-1}}$ (Caputo 1995, 1996; Caputo & Pavlides 1993). To the south, the tectonics are dominated by large faults striking WNW–ESE that dip either to the NE or to the SW, and are responsible for the formation of important basins such as the Gulf of Evia and the Gulf of Corinth (Mercier *et al.* 1976; Roberts & Jackson 1991). Microtectonic observations suggest that motion is diachronous on the same fault (Philip 1976). During the Pliocene, extension trended NE–SW as in Thessaly, but during the Quaternary this orientation changed to NNW–SSE with a small component of strike-slip motion on the faults.

There is strong evidence that continental Greece underwent extension with a direction variable in time. Most of the important tectonic structures are due to the NE–SW-trending Pliocene extension which generated basins bounded by faults striking NW–SE, but this extension changed to N–S or NNW–SSE during the Quaternary, and it is probably still active, as attested by seismicity. This change in the orientation is also seen on a few islands of the Northern Aegean Sea (Mercier *et al.* 1989; Pavlides & Tranos 1991) which are crossed by large strike-slip-motion active structures.

DATA

During the summer of 1992 (from July 1 until August 25), we operated a temporary network of portable stations covering southern Thessaly, Locrid, northern Evia and the islands of Skiathos, Skopelos and Alonissos. The purpose of this was to study the seismicity and focal mechanisms of the area and their consistency with the surface tectonic structures, especially for northern Evia and Locrid (Fig. 3). The network consisted of 68 stations, 62 of them recorded on smoked paper using 1 Hz vertical seismometers, and six of them Lennartz digital recorders connected to 1 Hz 3-D seismometers. The average spacing between stations was less than 15 km in order to ensure accurate estimations of the focal depths for crustal events and to allow a good coverage of first-motion polarities on the focal sphere. All internal clocks were calibrated periodically with a DCF radio telemetered time code, and we believe the time to be accurate to within 0.1 s. For the strongest events we also used the permanent stations of the University of Thessaloniki.

More than 9000 $P+S$ phases allowed us to locate 510 earthquakes recorded by more than four stations (Fig. 4). Details of the procedure used to determine the velocity structure and the Vp/Vs ratio, to locate the earthquakes and to select the most reliable events are discussed in Hatzfeld *et al.* (1990). The velocity structure for the Northern Aegean Sea differs from that for continental Greece (Table 1). The computed Vp/Vs ratio is 1.78. Among the earthquakes that we located, uncertainties in epicentre and depth for 318 of them were less than 5 km, and for 246 less than 2 km. The magnitude was calculated using the coda duration (Lee & Lahr 1972).

Focal mechanisms were computed for earthquakes that were recorded with more than eight first-motion polarities of upgoing rays. Among the 80 focal mechanisms, 22 (category A) had three quadrants sampled and the azimuth of both planes was constrained to within 10°, 27 (category B) had one plane constrained to within 10° and the other to within 20°. For the remaining 31 (Category C), we relaxed the criteria regarding the quadrants and therefore the fault planes varied by as much as 30° but they still gave an indication of the type of faulting (strike-slip, normal or reverse).

RESULTS

With a time span of only seven weeks, the few hundred events that we located may not be representative of the long-term deformation. Their virtue, however, lies in the fact that their locations are much more accurate than those recorded only by teleseismic or regional stations. To ensure that our data were representative, we smoothed our locations and mechanisms over a scale consistent with regional tectonics and compared our data with those of stronger (historical and teleseismically computed) events in the area. The magnitudes of the earthquakes ranged from 0.4 to 4.5 with a maximum number of events around magnitude 2.0. The depths of the earthquakes ranged between the surface and 34 km, but the great majority were located at a depth shallower than 15 km.

The lack of subcrustal seismicity, even over such a short period of time, concurs with the inference that the northern extent of Hellenic subduction lies largely south of our network. During a previous microearthquake study, we located some events at depths greater than 120 km beneath southern Evia (Hatzfeld *et al.* 1990). Reliable teleseismically located intermediate seismicity also stops beneath southern Evia (Hatzfeld & Martin 1991). Therefore, it is likely that intermediate-depth seismicity related to the Hellenic slab does not extend to the north of Evia.

The shallow seismicity is not uniformly distributed throughout the region. We observe a cluster associated with the North Aegean Trough, where the strongest event (magnitude 4.5) occurred during the experiment. We observe clusters also around the Gulf of Volos, the Pindus boundary, the Gulf of Evia and the Gulf of Corinth, which is located outside our network. Note the slight difference between locations from the International Seismological Center (NEIS) (Fig. 3) and our locations (Fig. 4), especially around Evia and east Locrid.

In the following, we describe our results in detail, region by region.

The North Aegean Trough and the Sporades Basin

This region lies outside our network. Because the strongest event ($Md > 4.5$) and the related aftershocks were also recorded by the permanent network of the Aristotle University of Thessaloniki, we could determine more precise locations than would have been possible with our network alone and we computed fault plane solutions for some of these events.

The seismicity is distributed in two main clusters (Figs 5 and 6). The northern cluster lies between the Sporades Basin and the Saros Trough. Relative to the surrounding high-bathymetry areas (Le Pichon *et al.* 1985), this trough is actually a very narrow and deep (greater than 6000 m) basin filled with Neogene sediments and constitutes the eastern termination of the Sporades Basin (Le Pichon *et al.* 1985). Seismic activity follows the direction of this narrow, deep basin and is consistent

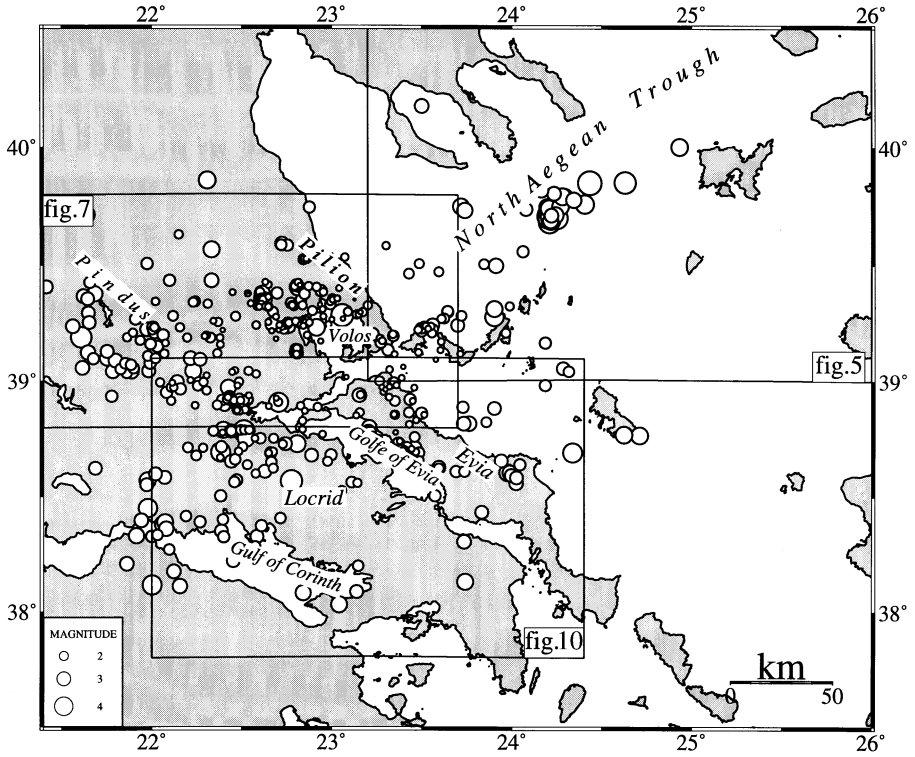

Figure 4. Map showing the 510 epicentres that we located with our temporary seismological network during the summer of 1992.

with the longer-term seismicity mapped with NEIS data. The focal mechanisms computed for the magnitude 4.5 earthquake of July 23 (#127) and its aftershocks (#128, 130, 131, 132, 142, 152) show strike-slip faulting. However, none of the fault planes is aligned with the direction of the deep bathymetry or basement. In general, one plane strikes almost E–W and dips north, whilst the other strikes N–S and dips west. The orientation of the E–W-striking plane is well determined because of the clear difference in polarities at stations located on the mainland. For the strike-slip events, the mechanisms differ only slightly from those computed for large earthquakes in the North Aegean Trough (Fig. 2) (Taymaz *et al.* 1991).

The southern cluster lies at the western border of the Sporades Basin, just north of Skopelos, where the deepest basin is located. The bathymetry is 1000 m but the basement is more than 10 000 m deep (Le Pichon *et al.* 1985). More precisely we can observe two subclusters. The first is located at the southern edge of the basin, with no clear shape, suggesting a single active fault. The second is located just north of the islands of Skiathos and Skopelos and crosses the NW–SE-striking faults inferred from the bathymetry (Lyberis 1984). We could not determine mechanisms for the first cluster because it is located outside our network, and the earthquakes were not strong enough to be recorded by the permanent stations. The earthquakes located north of Skiathos (#119, 121, 125, 159, 396, 440) clearly show strike-slip motion with one plane striking NE–SW, approximately parallel to the strike of the North Aegean Trough, and the other NW–SE, which differs by about 30° from the strikes of normal faults bounding the Pilion to the east. This seismicity pattern continues west towards the Gulf of Volos, but the style of faulting progressively changes to normal faulting (#24, 25, 141, 171, 425, 448) across the southern termination of the Pilion peninsula. Therefore, the strike-slip events are unlikely to be related to the important normal fault that bounds the Pilion area seawards and strikes NW–SE.

The Gulf of Volos and southern Thessaly

Most earthquakes in this region occurred either north of the Gulf of Volos or on the western border of the Karditsa Basin (Figs 7 and 8). We located no seismic activity that can be clearly related to the Larissa Basin or to the Pilion and its edges. The clear normal faults that dip eastwards and bound the SE edge of the Pilion were inactive during our experiment.

Around the Karditsa Basin, seismic activity is located at the western edge, where a strong (*M*s 7.0) earthquake occurred in 1954 and was associated with N–S extension (Papastamatiou & Mouyaris 1986). Most of this seismicity is restricted to the Pindus chain, whose western side is also quite active (Hatzfeld *et al.* 1995). The seismicity reveals no clear relation to the NW–SE-striking fault system that bounds the Karditsa Basin, and we could not compute focal mechanisms because these earthquakes were located outside the network.

North of the Gulf of Volos, the seismic activity is concentrated in two clusters. The first is clearly associated with the Nea Anchialos Fault system, which strikes E–W, dips southwards and bounds the northern edge of the Almyros Basin. This region experienced several strong earthquakes during historical time in 743 and 1773 according to Papazachos & Papazachou (1997), and in 1980 when a magnitude *M*s 6.5 event occurred. The foreshocks and aftershocks of the latter event are well aligned with the Nea Anchialos Fault and the focal mechanism indicates a N–S-trending extension along an E–W-striking fault (Papazachos *et al.* 1983). The distribution

Table 1.

Volos 1992, focal mechanisms

N°	Date & Time	Lat	Long	Z	Mag	Plan1		Plan2		P Axis		T Axis		Q
		°N	°E	km		Az	Pl	Az	Pl	Az	Pl	Az	Pl	
4	920707 8: 9	39.25	22.68	12.8	2.3	90.0	60.0	270.0	30.0	.0	75.0	180.0	15.0	A
9	920708 1:36	39.86	24.61	22.2	3.8	260.0	70.0	160.0	64.5	121.4	33.1	29.0	3.6	C
15	920709 9:49	38.96	23.13	10.3	2.5	250.0	60.0	140.0	59.4	105.3	45.6	14.9	.4	B
17	920709 17:31	39.57	22.74	12.0	2.7	105.0	30.0	280.0	60.1	183.3	74.8	11.8	15.1	B
21	920710 1:30	38.74	23.35	13.1	2.7	120.0	60.0	240.0	49.1	83.3	54.7	182.2	6.3	B
24	920710 16:28	39.19	23.34	11.0	1.9	200.0	60.0	95.0	65.9	55.5	40.0	148.6	3.7	B
25	920710 17:36	39.20	23.32	11.3	1.4	205.0	80.0	110.0	63.7	70.4	25.9	335.0	11.0	B
33	920711 17:49	39.39	22.94	10.1	2.1	80.0	45.0	270.0	45.4	262.5	85.0	355.0	.2	B
36	920711 21:13	39.38	22.95	10.4	1.5	90.0	50.0	310.0	47.6	292.9	68.6	199.6	1.3	C
37	920711 23:56	39.42	22.81	11.6	1.7	250.0	52.0	109.0	45.2	98.0	69.1	358.4	3.6	A
39	920712 1:46	39.42	22.81	10.6	1.4	95.0	40.0	275.0	50.0	185.0	85.0	5.0	5.0	C
45	920713 3:44	39.29	23.09	10.9	1.6	35.0	60.0	295.0	73.3	251.6	33.9	347.4	8.6	A
55	920714 12:35	38.91	22.49	11.7	1.9	90.0	60.0	270.0	30.0	.0	75.0	180.0	15.0	B
57	920714 21: 8	39.04	22.46	18.5	1.3	75.0	40.0	265.0	50.4	214.0	82.8	350.5	5.2	C
61	920715 0:34	39.26	22.85	8.9	1.3	95.0	55.0	280.0	35.1	353.5	79.8	187.1	10.0	C
66	920715 8:29	39.01	23.25	10.3	1.8	275.0	35.0	95.0	55.0	5.0	80.0	185.0	10.0	B
76	920716 11:58	38.76	23.34	12.8	2.2	70.0	75.0	165.0	72.0	117.9	2.0	27.0	23.7	B
79	920716 22:12	39.11	23.34	12.1	1.3	60.0	45.0	290.0	57.3	254.5	61.9	357.3	6.8	C
81	920717 2: 8	39.35	23.02	8.4	1.2	300.0	87.0	35.0	31.0	238.3	40.0	3.8	34.7	C
99	920718 19:45	38.86	23.35	12.1	1.6	120.0	65.0	225.0	61.0	81.2	39.9	173.3	2.5	A
110	920721 11: 8	38.99	23.34	9.4	1.2	120.0	60.0	225.0	65.9	84.5	40.0	351.4	3.7	B
111	920721 15:13	38.70	23.34	12.8	2.3	120.0	60.0	245.0	45.2	81.7	58.4	185.5	8.3	A
119	920722 21:42	39.21	23.47	11.0	2.0	245.0	75.0	340.0	72.0	292.9	2.0	202.0	23.7	B
120	920722 21:43	38.76	23.26	10.1	1.7	55.0	60.0	310.0	65.9	270.5	40.0	3.6	3.7	B
121	920722 22:27	39.22	23.49	10.8	1.7	245.0	75.0	340.0	72.0	292.9	2.0	202.0	23.7	B
123	920723 3:35	38.78	23.44	11.7	1.8	110.0	80.0	205.0	63.7	64.6	25.9	160.0	11.0	B
125	920723 12:41	39.23	23.54	10.5	2.3	155.0	60.0	250.0	81.4	116.6	27.3	19.0	14.4	A
127	920723 20:12	39.82	24.43	18.0	4.5	270.0	50.0	167.0	75.0	120.2	39.6	223.7	15.7	A
128	920723 20:18	39.82	24.35	19.5	4.0	255.0	80.0	160.0	63.7	120.4	25.9	25.0	11.0	C
130	920723 20:23	39.81	24.37	19.3	3.4	80.0	80.0	345.0	63.7	305.4	25.9	210.0	11.0	C
131	920723 20:24	39.80	24.40	20.5	4.0	80.0	80.0	345.0	63.7	305.4	25.9	210.0	11.0	C
132	920723 20:37	39.83	24.37	25.9	3.3	80.0	80.0	345.0	63.7	305.4	25.9	210.0	11.0	C
141	920724 1: 6	39.16	23.24	11.4	2.0	130.0	50.0	245.0	63.3	104.4	50.6	4.7	7.8	A
142	920724 1:12	39.83	24.37	25.6	3.2	40.0	50.0	295.0	72.9	249.3	41.5	352.3	14.2	C
152	920724 23:46	39.82	24.39	19.5	3.7	260.0	70.0	165.0	76.5	121.4	24.0	213.4	4.4	C
159	920726 1:50	39.24	23.69	10.1	2.3	60.0	70.0	320.0	64.5	281.4	33.1	189.0	3.6	C
171	920727 19: 7	39.21	23.21	11.4	2.4	70.0	45.0	330.0	80.1	278.9	38.4	27.9	22.3	A
173	920728 10:33	38.87	23.49	13.5	2.3	230.0	80.0	135.0	63.7	95.4	25.9	.0	11.0	C
180	920729 7:51	38.70	22.90	11.7	2.3	240.0	70.0	140.0	64.5	101.4	33.1	9.0	3.6	B
183	920729 11: 0	38.98	22.44	13.7	2.9	90.0	50.0	290.0	41.8	301.6	79.1	189.3	4.2	A
191	920730 16:46	39.33	22.78	10.5	2.0	265.0	60.0	110.0	32.5	144.1	71.8	4.5	14.1	C

of the microearthquakes confirms that the Nea Anchialos Fault continues eastwards across the Pilion as proposed by Caputo (1996). A N–S-trending section (Fig. 9a) across the fault shows south-dipping activity down to 10 km.

The second cluster is located near the region of Velestino, where an earthquake of magnitude 6.8 and two others of magnitude greater than 6.0 occurred within 12 hr in 1957 (Papazachos & Papazachou 1997). No ground rupture was observed, and there was no obvious evidence relating this earthquake to any fault, even though the Righeo Fault could be a good candidate (Caputo 1990). Our seismicity splits into two clusters that align approximately E–W. Because there are many faults striking E–W in this area such as the Velestino, the Righeo, the Vassilika and the Nea Pagasae faults (Caputo 1990), it is difficult to relate our seismicity to any of those structures. Nevertheless, the Nea Pagasae Fault seems to be the most plausible because the dip of the structure fits the distribution of the earthquakes located at about 5 km depth (Fig. 9b).

The Nea Anchialos and Nea Pagasae faults are E–W-striking antithetic normal faults. The better-constrained focal mechanisms (#4, 209, 356), as well as the less well-constrained solutions (#61, 208, 215, 421) associated with the Nea Anchialos Fault indicate E–W-striking normal faulting. We obtained a similar pattern for the focal mechanisms associated with the Nea Pagasae Fault (#33, 37, 297, 383, 386, 389, 398). In conclusion, it seems clear that this area is under N–S extension along a set of E–W-striking parallel faults. It is worth noting that a few events, located to the east, exhibit a slight component

Table 1. (*Continued.*)

Volos 1992, focal mechanisms															
N°	Date & Time		Lat	Long	Z	Mag	Plan1		Plan2		P Axis		T Axis		Q
			°N	°E	km		Az	Pl	Az	Pl	Az	Pl	Az	Pl	
196	920730	20: 5	38.90	22.92	13.5	1.6	160.0	70.0	255.0	76.5	118.6	24.0	26.6	4.4	A
207	920731	16:54	38.79	23.22	10.9	1.6	120.0	75.0	215.0	72.0	77.0	23.7	167.9	2.0	B
208	920731	20:26	39.24	22.72	10.1	1.6	80.0	60.0	260.0	30.0	350.0	75.0	170.0	15.0	C
209	920731	20:29	39.24	22.72	6.7	1.5	80.0	60.0	260.0	30.0	350.0	75.0	170.0	15.0	B
215	920801	2:32	39.25	22.88	7.2	1.3	90.0	50.0	305.0	45.7	293.7	71.5	196.9	2.3	C
226	920804	5:47	38.69	22.68	12.1	2.1	105.0	60.0	280.0	30.1	21.8	74.9	193.2	15.0	B
254	920806	14:45	38.92	23.43	13.8	2.3	284.0	85.0	192.0	68.3	56.1	11.6	150.1	18.9	A
262	920807	6:16	39.40	22.91	9.0	1.6	290.0	70.0	60.0	29.5	231.2	59.0	3.3	21.9	C
265	920807	10:39	38.91	22.50	10.8	1.9	265.0	40.0	123.0	56.5	83.4	68.7	196.6	8.7	C
267	920807	19:44	38.67	23.37	11.4	1.7	120.0	60.0	220.0	73.3	83.4	33.9	347.6	8.6	C
271	920808	4: 0	38.92	22.42	9.9	2.1	155.0	70.0	280.0	32.4	99.8	57.0	225.6	20.8	C
273	920808	9:30	38.91	22.40	12.2	1.8	175.0	70.0	280.0	54.6	132.2	40.7	230.6	9.7	A
277	920808	22:26	38.98	22.47	14.9	1.2	95.0	52.0	257.0	39.4	51.8	79.0	177.0	6.4	C
279	920809	5: 9	38.90	23.69	12.1	2.1	145.0	50.0	250.0	72.9	115.7	41.5	12.7	14.2	A
282	920809	14:32	39.01	23.34	7.3	1.6	120.0	50.0	230.0	67.8	92.7	46.2	351.2	10.8	B
286	920809	19: 1	39.40	22.81	11.6	2.1	233.0	80.0	130.0	38.1	107.6	42.8	351.1	25.7	A
295	920810	11:58	39.40	22.81	10.3	2.4	110.0	50.0	250.0	47.6	87.1	68.6	180.4	1.3	C
297	920810	14:42	39.37	22.85	10.8	2.0	280.0	40.0	105.0	50.1	38.8	84.4	192.7	5.1	B
329	920813	16:26	38.71	22.67	13.7	2.2	95.0	55.0	275.0	35.0	5.0	80.0	185.0	10.0	A
334	920814	5:41	39.41	22.80	11.8	1.6	295.0	35.0	100.0	55.9	341.6	77.3	196.1	10.5	C
341	920815	1:47	38.75	22.76	12.9	2.5	100.0	35.0	275.0	55.1	173.6	79.7	7.1	10.1	A
342	920815	3:20	38.74	22.75	13.4	1.6	85.0	55.0	265.0	35.0	355.0	80.0	175.0	10.0	B
356	920817	16:54	39.28	22.95	8.0	1.1	210.0	25.0	100.0	80.9	35.2	48.8	170.7	32.0	A
360	920818	3:39	38.64	23.53	12.5	1.8	290.0	65.0	190.0	69.6	240.8	3.0	148.9	33.1	B
383	920819	20:15	39.34	22.63	12.1	2.7	85.0	40.0	270.0	50.1	203.8	84.4	357.7	5.1	A
386	920819	21:20	39.35	22.62	12.6	1.8	70.0	65.0	320.0	53.7	289.8	45.8	192.7	6.9	A
388	920819	22:11	39.35	22.63	11.2	2.0	110.0	25.0	260.0	68.0	149.4	64.9	359.3	22.1	C
389	920819	23:11	39.36	22.62	11.7	1.7	100.0	40.0	230.0	61.7	93.5	61.3	340.8	11.9	B
394	920820	10:36	38.88	23.39	11.6	1.8	210.0	65.0	95.0	47.8	71.5	50.7	328.8	10.1	B
396	920820	15:25	39.21	23.55	14.5	1.6	95.0	35.0	205.0	76.5	80.2	48.1	319.8	24.5	B
398	920821	1:59	39.36	22.62	11.1	1.8	70.0	40.0	285.0	55.5	246.1	70.4	359.7	8.1	B
402	920823	2: 2	39.30	23.16	8.1	1.6	140.0	65.0	230.0	90.0	97.8	17.4	2.2	17.4	C
407	920823	9:36	38.81	23.20	14.1	2.8	113.0	60.0	215.0	70.2	76.9	36.4	342.1	6.5	A
421	920823	22: 6	39.26	22.79	5.8	1.5	65.0	70.0	320.0	54.6	287.8	40.7	189.4	9.7	C
425	920824	1:22	39.19	23.25	11.3	1.3	255.0	30.0	60.0	60.9	311.7	73.1	155.5	15.5	C
426	920824	1:28	38.58	23.12	14.8	2.1	130.0	65.0	235.0	61.0	91.2	39.9	183.3	2.5	C
440	920824	11:35	39.22	23.56	10.9	1.7	275.0	70.0	10.0	76.5	233.6	24.0	141.6	4.4	B
448	920824	23:52	39.14	23.30	11.4	2.2	340.0	75.0	245.0	72.0	112.1	2.0	203.0	23.7	A
452	920825	2:31	39.28	23.13	7.3	1.6	130.0	60.0	280.0	33.7	75.7	70.4	208.4	13.6	C

of strike-slip motion, which is consistent with the events recorded in southern Pilion.

Locrid and northern Evia

One of the major goals of our experiment was to investigate the seismicity located south of the Gulf of Volos (Figs 10 and 11). This region experienced very strong earthquakes in historical time, in 426 BC, in 1740 and more recently in 1894. This most recent event, known as the Atalanti-Martinon earthquake, was composed of two shocks of magnitudes 6.5 and 6.7, a week apart. Remnant surface breaks that are still visible today show normal faulting with the reactivation of the N300°-striking fault (Ambraseys & Jackson 1990). However, instrumental seismicity (even located by the regional VOLNET seismological network operated by the University of Athens) does not show any seismicity associated with this fault. Due to the impressive normal faults observed along Kallidromon and Kamena Vourla for several tens of kilometres (Philip 1976; Lemeille 1977), this lack of seismicity can be interpreted as a seismic quiescence period between major earthquakes.

Important seismicity is located around the Lamia Basin, the Renginion Basin and northern Evia. The microseismicity shows a diffuse pattern that cannot be directly associated with any specific fault such as the Kamena Vourla or Kallidromon faults, but seismic activity unquestionably occurs as deep as 15 km. Minor activity occurred around the Atalanti-Martinon Fault. The earthquakes located beneath northeastern Evia are unlikely to be associated with any of the known surface faults, because the western Kandili Fault dips westwards and the eastern Evia Fault dips eastwards and therefore away from the seismic activity (Fig. 9c).

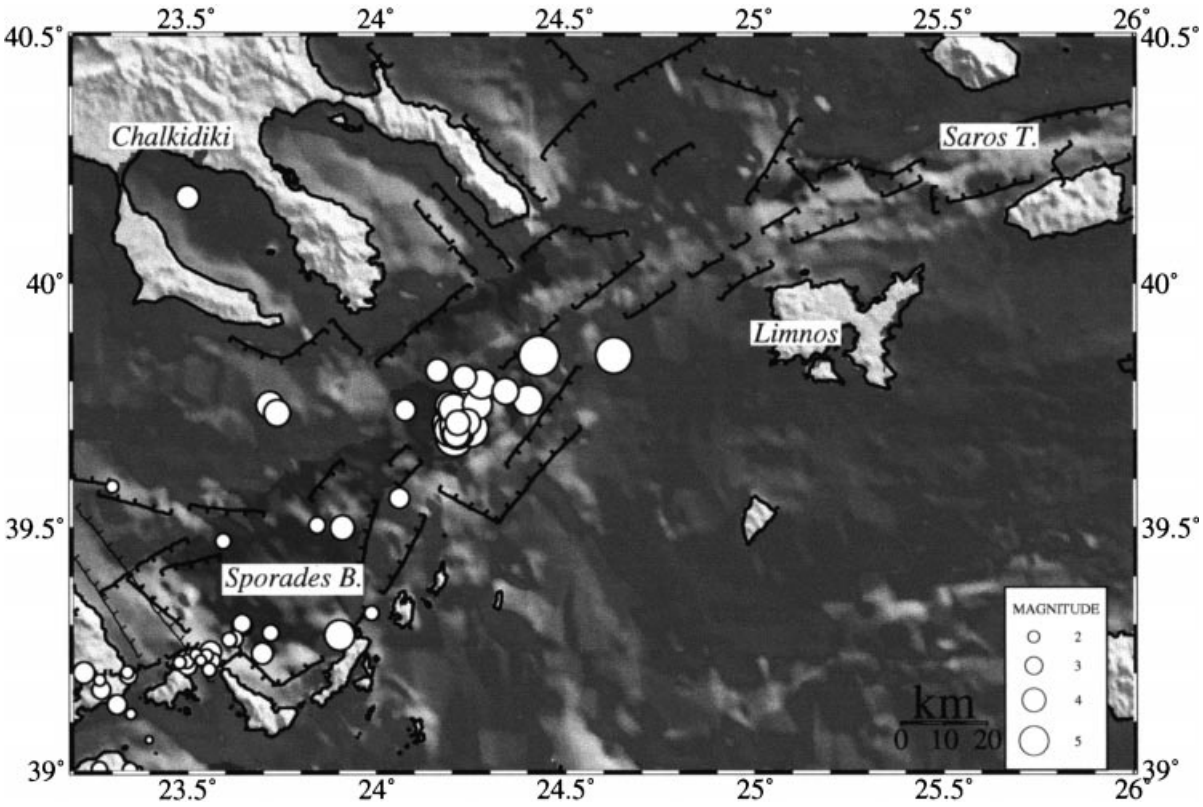

Figure 5. Seismicity map of the northern Aegean sea showing the reliably located earthquakes with uncertainties smaller than 5 km and recorded by more than eight stations. The major faults are shown with heavy and thin lines for the Quaternary and Pliocene structures, respectively (after Mercier *et al.* 1976; Roberts & Jackson 1991; Caputo & Pavlides 1993).

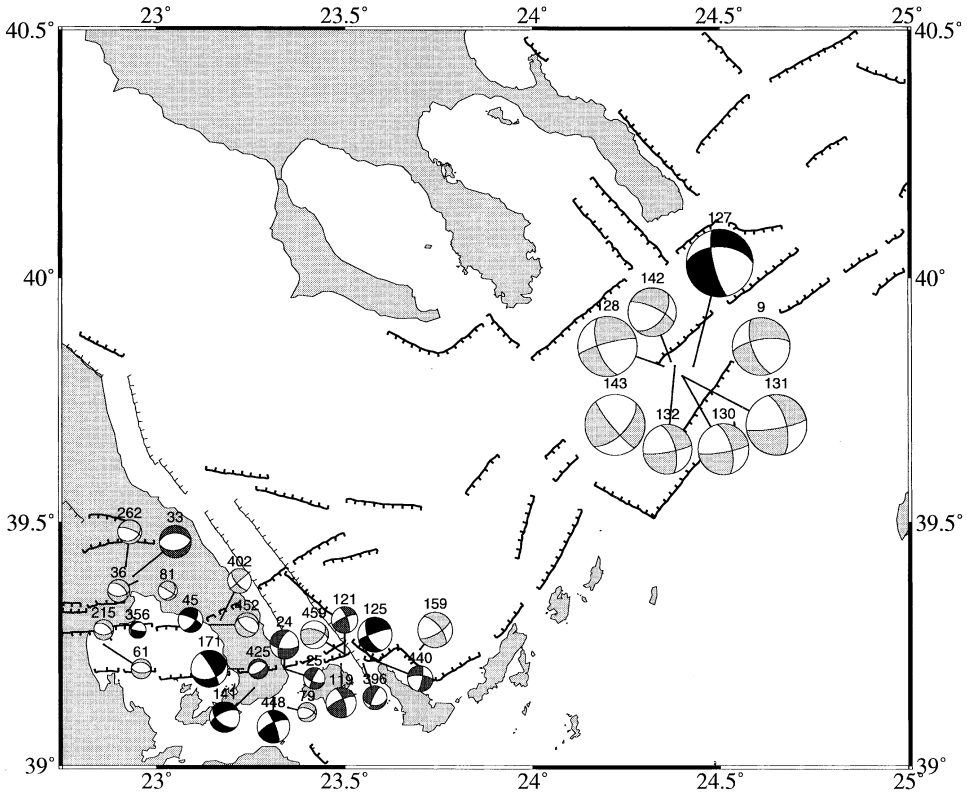

Figure 6. Map showing focal mechanisms computed for the northern Aegean. Solid quadrants include compressional first motion; open quadrants show dilatations. Black quadrants indicate category 1 mechanisms with two planes well constrained; dark grey category two mechanisms with one plane well constrained; light grey category 3 mechanisms. We note that the dextral strike-slip motion along the North Aegean Trough progressively transfers into pure normal faulting on E–W-striking planes and N–S extension around the Gulf of Volos.

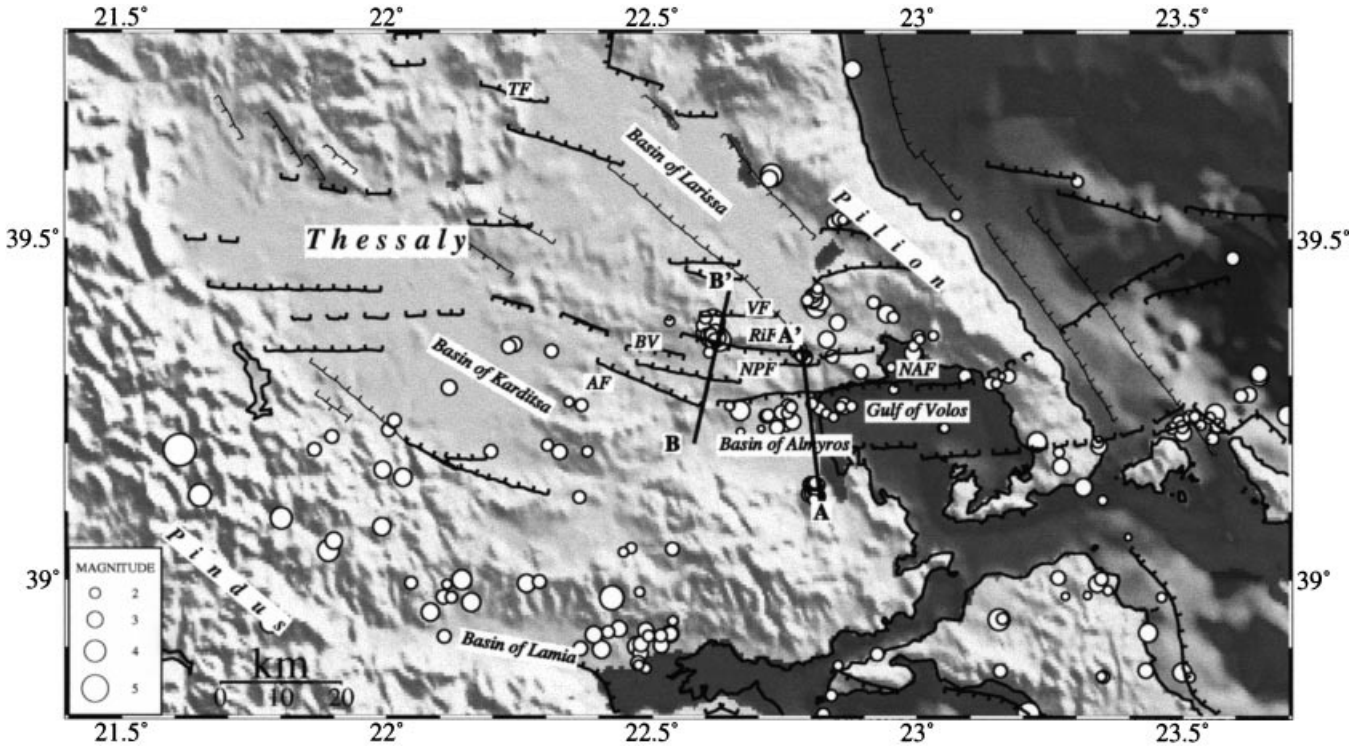

Figure 7. Seismicity map of the reliably located earthquakes in Thessaly and the Gulf of Volos. No earthquakes are located along the NW–SE-striking faults that bound the Pilion to the east and the Larissa Basin. The major faults are reported with the same convention as in Fig. 4. VF: Velestino; RiF: Righeon; BV: Vassilika; NPF: Nea Pagasae; TF: Tyrnavos; NAF: Nea Anchialos; AF: Ambelia. Seismicity is associated with the Nea Anchialos Fault, the Velestino Fault system and the Lamia Basin. The locations of the cross-sections A–A′ and B–B′ are also shown (Fig. 9).

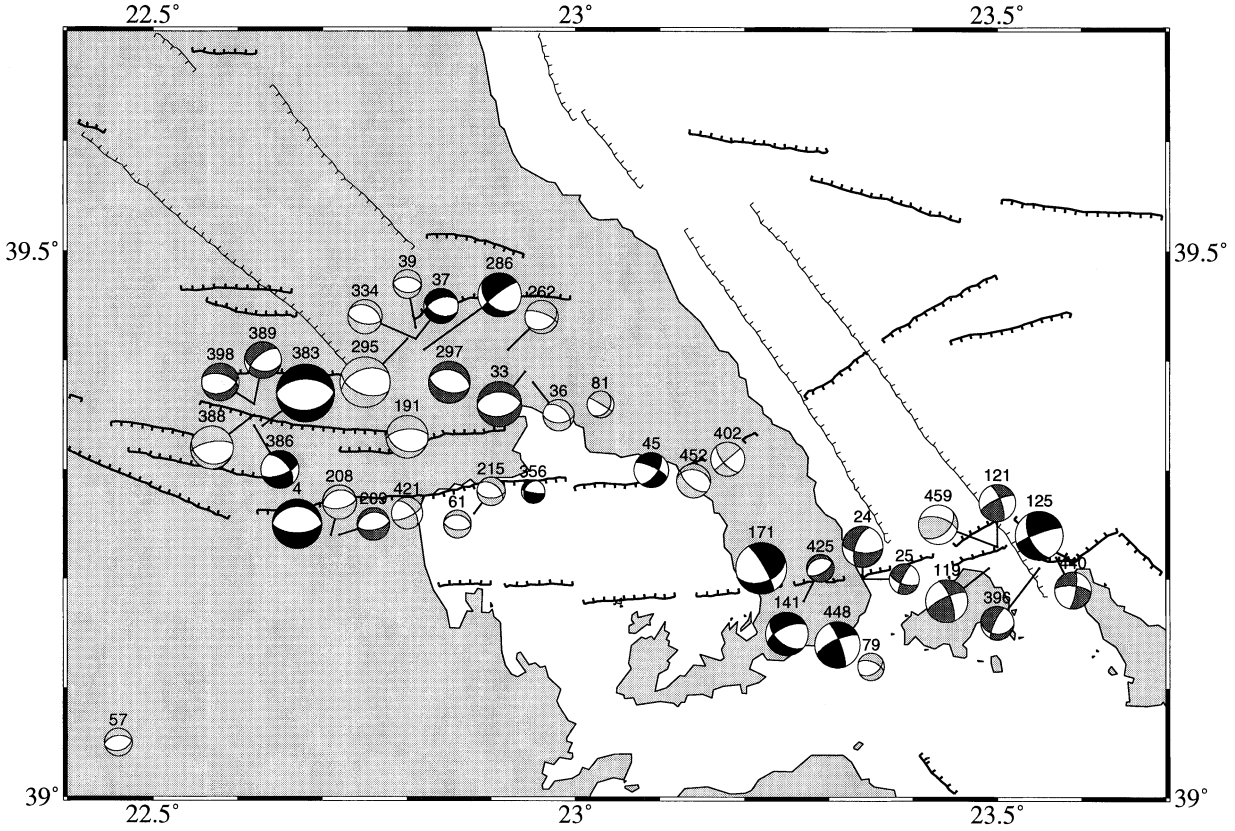

Figure 8. Map of the focal mechanisms computed for Thessaly and the Gulf of Volos (symbols as in Fig. 5). Note the transition from dextral strike-slip motion around the island of Skiathos to the N–S-trending pure extension along the Nea Anchialos Fault.

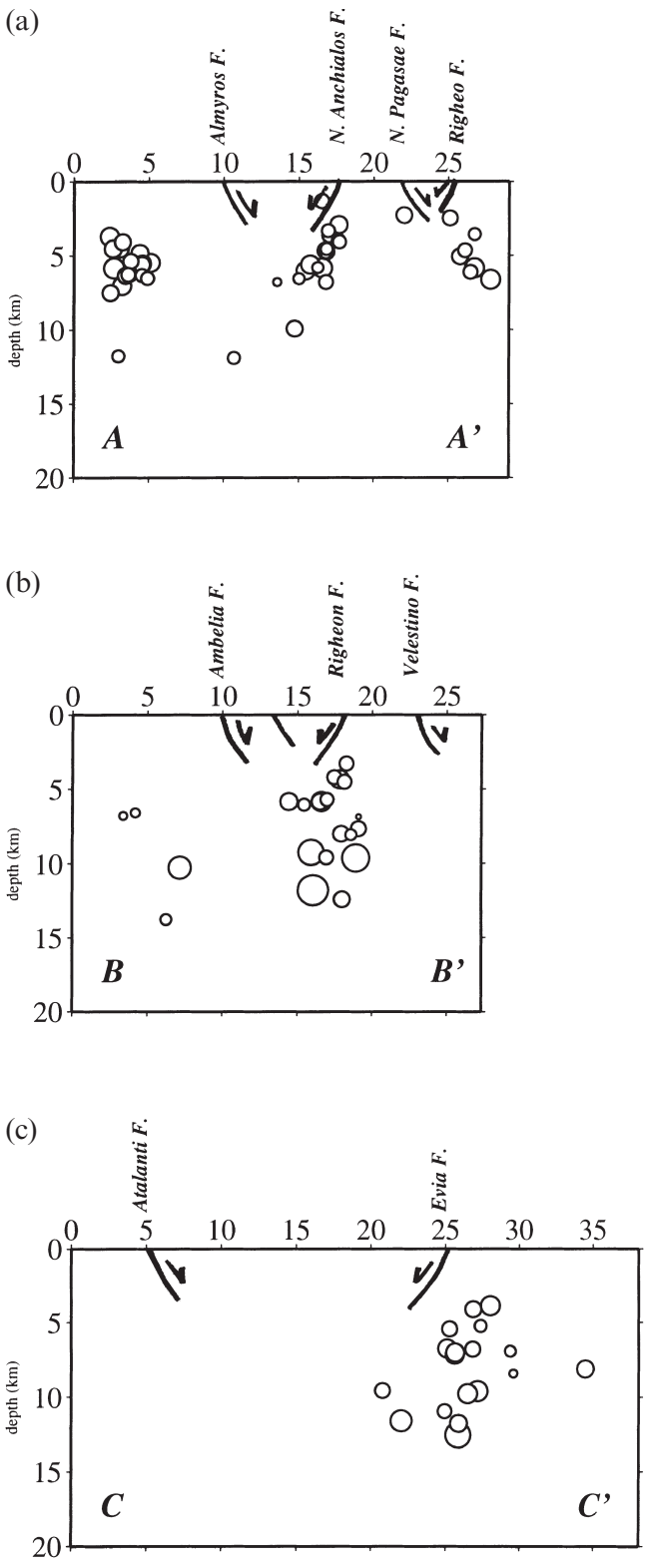

Figure 9. Cross-sections across (a) the Almyros Basin, suggesting that the Nea Anchialos Fault is active, (b) the Vassilika Basin and (c) the Gulf of Evia, which do not show a clear pattern of seismicity associated with specific faults.

The focal mechanisms show two distinct patterns. Beneath the Lamia Basin, west of the city of Lamia (#55, 57, 183, 265, 277) and close to the Kallidromon, the Kamena Vourla faults and the Renginion Basin (#226, 329, 341, 342), mainly normal faulting along E–W-striking faults is observed. However, in northern Evia focal mechanisms (e.g. #99, 254, 279, 407) indicate strike-slip faulting with T-axes trending approximately N–S. We have found no evidence that the same occurs along the Atalanti-Martinon Fault (#180, 425). Therefore, although all the T-axes are oriented approximately N–S, parallel to the regional extension (Mercier *et al.* 1989; Caputo & Pavlides 1993), the two different types of focal mechanisms (normal and strike-slip) suggest that individual blocks are limited by inherited faults.

DISCUSSION

The pattern of microseismicity that we obtained from seven weeks of recording shows some common features and some differences compared to the instrumental seismicity map provided by NEIS locations (Fig. 1), the historical seismicity (Fig. 2, Papazachos & Papazachou 1997) and the most important faults.

On all maps, we see seismic activity along the North Aegean Trough, around the Gulf of Volos and west of the Karditsa Basin. In some places (e.g. the North Aegean Trough or the Nea Anchialos Fault) the seismicity is associated with known active (or very recent) faults. In some areas (e.g. Velestino-Nea Pagasae system) activity is not clearly associated with specific faults, and in one case (the Lamia Basin) our precisely located earthquakes cannot be associated with any mapped fault. This observation implies that brittle deformation is not confined to important individual surface faults, but is distributed over broad areas or associated with hidden faults.

On the other hand, some important tectonic features are not related to any seismic activity. This is especially true for most of the large NW–SE-striking faults such as that to the east of Pilio, in Locrid, or those bounding the Karditsa and Larisa basins where Pliocene activity has been documented (Caputo 1990).

We will describe in more detail a few regions of particular interest.

The eastern Pilion

We did not locate any earthquake along the NW–SE-striking normal faults that bound to the east the Pilion region and to the west the Sporades Basin (Fig. 7). Also, we did not observe any significant seismic activity along the eastern coast of Evia (Fig. 10). This is also true for instrumental and historical seismicity. Therefore, these faults seem seismically inactive at the present time, even though they were important active features during the Pliocene. According to most of the proposed models of the geodynamic evolution of the Northern Aegean, the Sporades Basin is an important extensional feature bounded to the west by an active fault (Taymaz *et al.* 1991; Dinter & Royden 1993; Jolivet *et al.* 1994; Armijo *et al.* 1996). However, no seismological evidence of such a NW–SE-striking active normal fault is found in the historical seismicity or in our data.

In contrast, microseismicity is located in areas that were inactive on instrumental seismicity maps (Fig. 10). In particular,

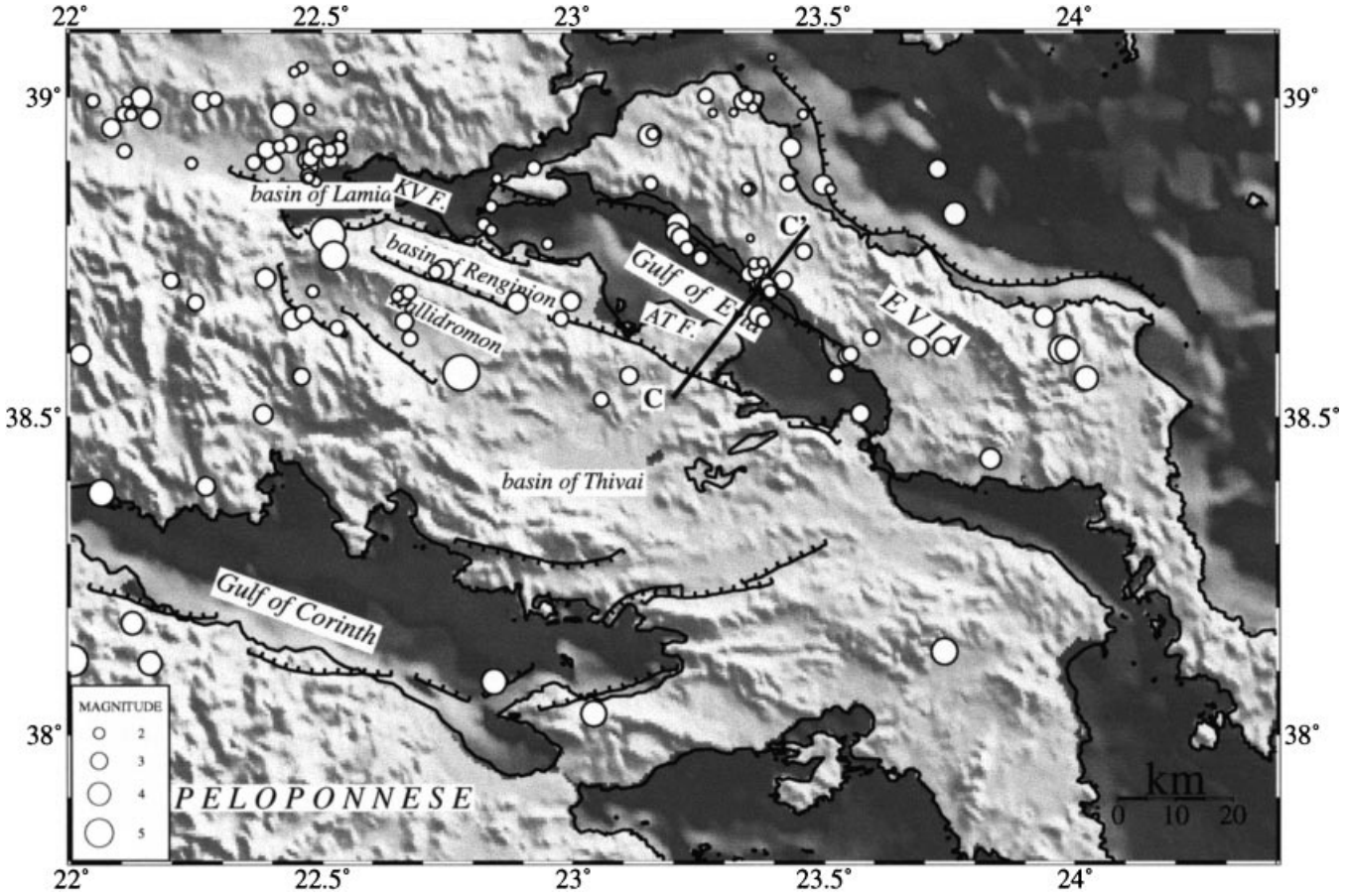

Figure 10. Seismicity map of the reliably located earthquakes in Evia and Locrid. Same symbols and references as in Fig. 4. Little seismicity is associated with the Kamena Vourla Fault (KVF) and Atalanti Fault (ATF). Most of the seismicity is located around the Lamia Basin and spread over Locrid and northern Evia. The location of the cross-section C–C′ is also shown.

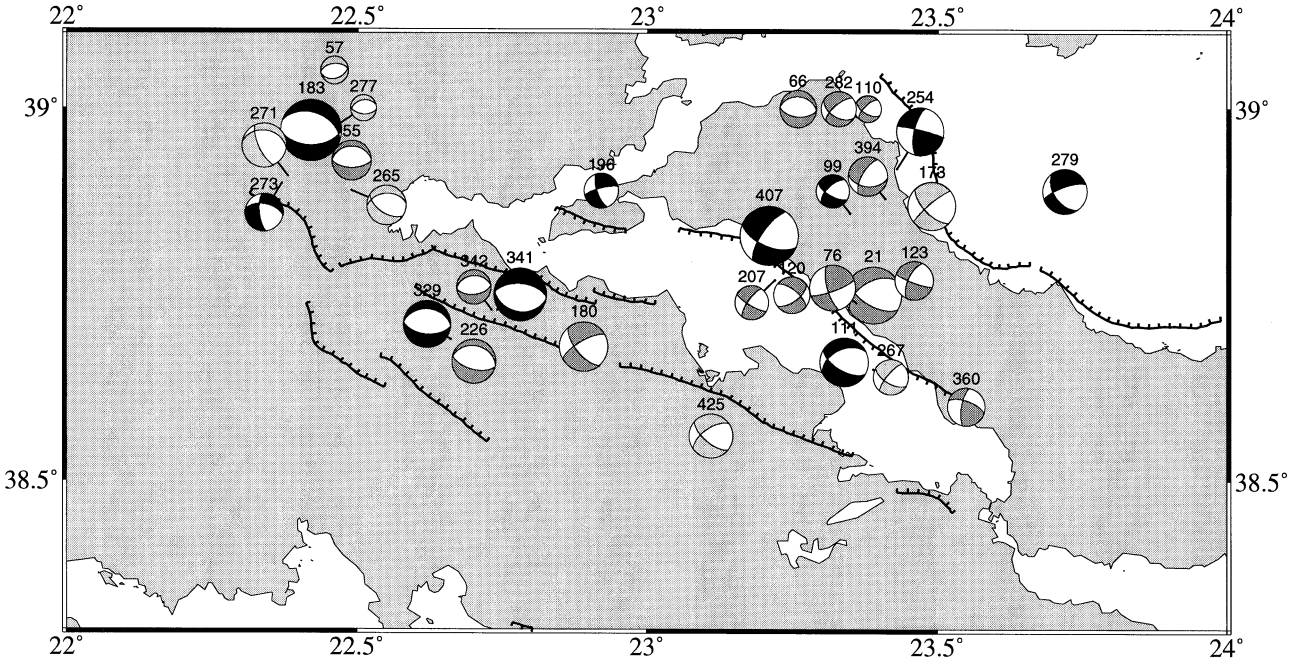

Figure 11. Map of the focal mechanisms computed for Evia and Locrid. Strike-slip motion is observed in Northern Evia, but N–S extension within the Lamia Basin.

we located earthquakes around the Gulf of Lamia (especially west of it) and around northern Evia. Several strong earthquakes destroyed the city of Lamia in 1740 and 1758 (Papazachos & Papazachou 1997).

North Aegean–Nea Anchialos

The seismic activity of the NE–SW-trending North Aegean Trough connects with the E–W-striking Almyros–Nea Anchialos system of antithetic normal faults (Figs 5 and 7) and crosses the Pilion peninsula almost orthogonally. During our experiment, only the Nea Anchialos Fault (which is related to the 1980 earthquake) was active, but both show similar recent tectonic activity (Caputo 1996). Clearly, the dextral strike-slip motion along the NE–SW-trending fault zone of the North Aegean Trough progressively changes into pure N–S extension along E–W-striking fault systems (Fig. 8). This pattern of deformation offers no evidence for oblique-slip or normal faulting on NW–SE-trending 'slats', as proposed by Taymaz *et al.* (1991). Instead, N–S-trending extension seems to occur on a new generation of normal faults striking E–W (such as the Ambelia-Vassilika or Nea Pagasae-Righeo faults) which strike perpendicular to the main active faults (Caputo & Pavlides 1993). A similar pattern, with transfer of motion, has been observed around the Mygdonian Graben located further north at the western termination of the Kavala Fault (Hatzfeld *et al.* 1987).

Northern Evia and the Gulf of Lamia

In Northern Evia, microseismicity is associated with strike-slip faulting (Fig. 11), but no strike-slip faults have been mapped in this area. Therefore, the question of whether our mechanisms represent dextral strike-slip on E–W-striking faults, or sinistral on NW–SE-striking faults remains open and we have two possible explanations. (1) The North Aegean Trough continues into the E–W-trending Gulf of Lamia, which is a subsiding basin that cuts the Pindus chain, and there is a progressive transfer (as is the case for the Nea Anchialos region) of dextral strike-slip motion into normal faulting. The Lamia Basin has been considered as a possible transfer zone (the 'Sperchios corridor') between the North Aegean Trough and the Kefallinia strike-slip fault (Mercier *et al.* 1979). (2) The NW–SE-striking faults in northern Evia have left-lateral strike-slip mechanisms on a plane that is parallel to the direction of the Kallidromon, Kamena-Vourla and Kandilli normal faults. These faults behaved as pure normal faults during the Middle Pliocene under NNE–SSW-trending extension, but were reactivated with a left-lateral oblique component under Quaternary NNW–SSE-trending extension (Mercier *et al.* 1976).

ACTIVE FAULTS AND KINEMATICS

In summary, we find seismic activity along NE–SW-striking dextral strike-slip faults within the Aegean Sea, connected to E–W-striking systems of normal faults in mainland Greece. None of the models that have been proposed for this region fits our data. For example, the 'broken slat model' of Taymaz *et al.* (1991) shows similar features such as strike-slip motion along the three different branches of the North Aegean Trough, and an abrupt change in the slip vectors around 23°E longitude. In contrast, the seismically active structures west of 23°E do not strike NW–SE as they proposed but E–W; for example, the Nea Anchialos Fault, the Velestino Fault or the Gulf of Lamia structure.

The model of a westward-propagating tip of the southern branch of the Northern Aegean Trough (Armijo *et al.* 1996) suggests strong similarities among the tectonics that affect the Gulf of Corinth, the Gulf of Evia and the northern Evia Basin. However, the present-day seismicity and fault plane solutions are different in the Gulf of Corinth, the Sporades Basin and the Gulf of Evia.

Our data show that the two northern branches of the Northern Aegean Trough are connected westwards to purely extensional features that trend more E–W across mainland Greece. This is also the case for the Kavala Fault in Eastern Macedonia, which strikes parallel to the North Aegean Trough and is connected to the E–W-trending Mygdonian Basin. Some E–W-striking extensional features similar to the Lamia Basin or the Almyros Basin exist further west, such as the Trikhonis Lake and the Ambrachikos Gulf, and could constitute a diffuse zone of N–S-trending extension connecting the North Aegean Trough to the Hellenic subduction. This resembles the 'bookshelf' model proposed by McKenzie & Jackson (1983) and Jackson & McKenzie (1984), in which blocks such as Evia are located within a transfer shear zone and rotate clockwise. Palaeomagnetic studies confirm such rotations (Kissel *et al.* 1986). Thus all the strike-slip motion on the two northern branches of the North Aegean Trough, as on the Kavala Fault, terminates with E–W-striking normal faults (Fig. 12). Indeed, the development of E–W normal faults post-dates the NW–SE-striking faulting that originated during Pliocene time and that is more visible in Thessaly (Caputo & Pavlides 1993), east of Pilio (Armijo *et al.* 1996) and in Macedonia (Mercier *et al.* 1983).

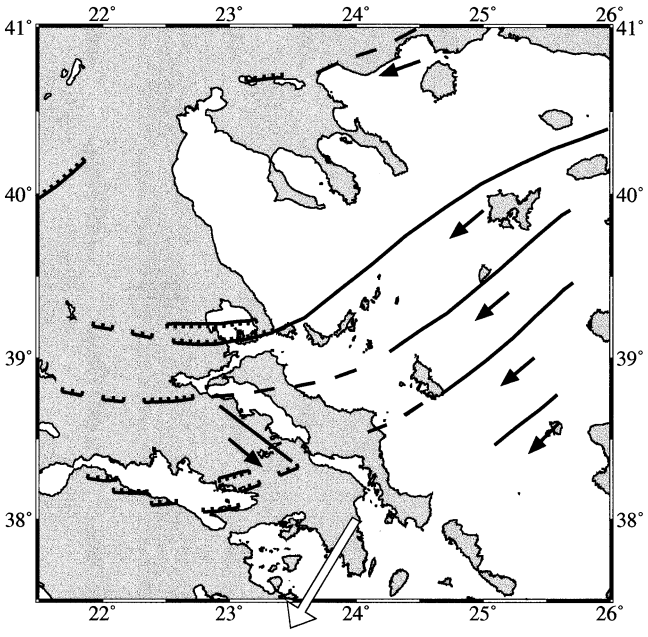

Figure 12. Schematic map of active faults affecting Central Greece. We assume a fault to be active when related to seismic activity (historical, teleseismically located or microseismic) and all the other faults to be inherited from the Pliocene tectonics but not active anymore.

Slip vectors represent the slip on faults that separate blocks. The pattern of slip vectors deduced from our focal mechanisms is rather complex (Fig. 13). It describes the large-scale kinematics only if all the faults are sampled and if the blocks are not deformable. In the North Aegean Sea where the blocks are of large scale, the slip vectors trend approximately parallel to velocities determined using GPS (Davies *et al.* 1997). This is not the case in mainland Greece, where crustal blocks are numerous and perhaps deform.

STRAIN PATTERN

The distribution of the T-axes (Fig. 14) as deduced from our fault plane solutions is consistent with the mechanisms of stronger earthquakes computed by body wave modelling (Taymaz *et al.* 1991) and CMT solutions (Harvard) in places where we have both. Therefore, we think that our microearthquake mechanisms are representative of large-scale deformation. They show that the main mechanism of deformation is N–S-trending extension all over the area, with a significant orthogonal component of horizontal shortening in the Northern Aegean Sea associated with strike-slip faulting. This strain pattern is consistent with that deduced from SLR measurements (Robbins *et al.* 1994; Noomen *et al.* 1995) and with GPS geodetic observations (Billiris *et al.* 1991; Davies *et al.* 1997), particularly regarding the N–S strain extension that affects the Lamia Basin and the strike-slip motion that affects the northern Evia and Locrid regions (NNE–SSW extension and WNW–ESE shortening). It is also worth noting that the geodetic strain computed over a 100 yr time period (Davies *et al.* 1997) shows that most of the N–S extension is located around the Gulf of Corinth and north of it, and that the strain is smaller in Attiki, between the Gulf of Corinth and the Gulf of Evia, which is consistent with a smaller seismic

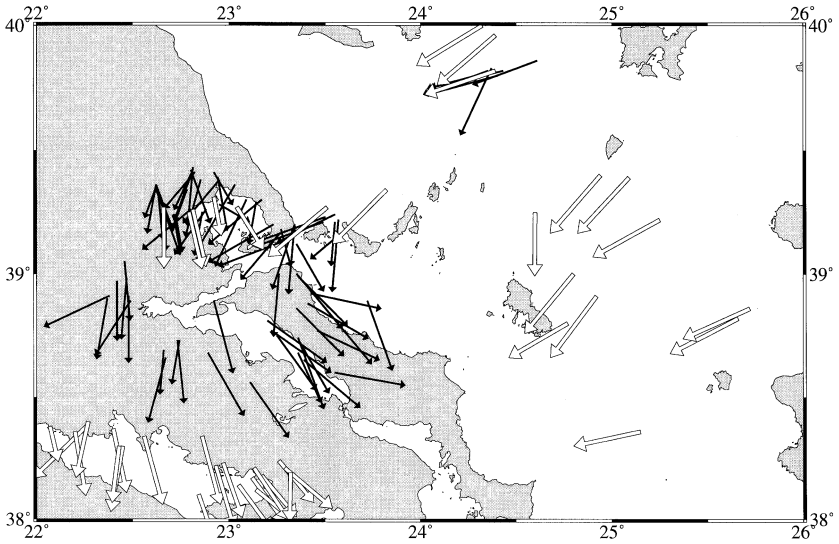

Figure 13. Map of the slip vectors obtained from the focal mechanisms. We assume the inferred fault plane from tectonic information (see text). Arrows show the motion of the southern block relative to the northern one. Thin solid arrows are from microearthquakes, large open arrows from larger events (Taymaz *et al.* 1991; CMT solutions). Note the complex pattern of slip vectors that may represent the motion between blocks.

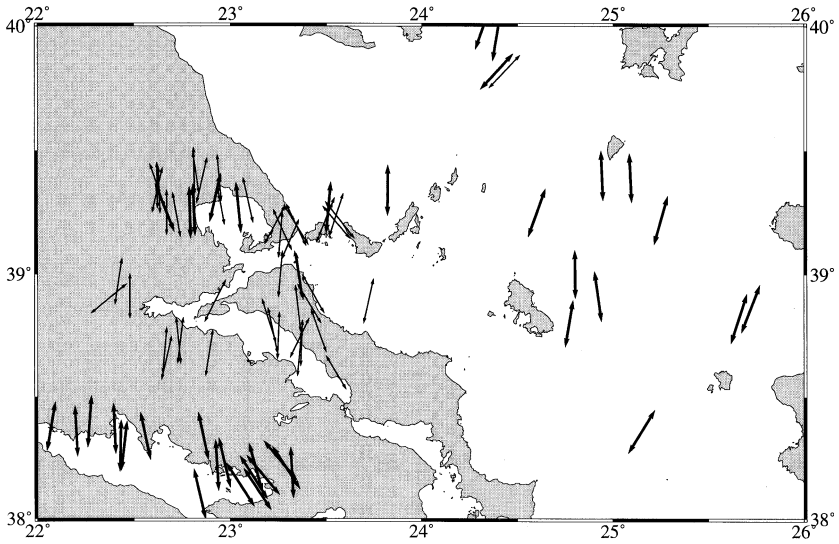

Figure 14. Map of the T-axes of the focal mechanisms, which show a very consistent N–S extensional pattern all over the area and are consistent with the strain as deduced from geodetic observations (Billiris *et al.* 1991; Davies *et al.* 1997; Noomen *et al.* 1995).

energy release there. As suggested by Pavlides & Caputo (1994), if the tectonics were related to the westward push of Turkey along the North Anatolian Fault and the North Aegean Trough, we would observe E–W compressional features, trending perpendicular to the motion, but this is seen only in western Greece where continental collision occurs. On the other hand, the consistent orientation of T-axes, both for the strike-slip structures of the North Aegean Sea and for the E–W-striking normal faults in mainland Greece, supports the idea that part of the present geodynamics of the Aegean is governed by buoyancy forces due to differences between continental and oceanic lithosphere across the Hellenic Trench southwest of the Peloponnese (Le Pichon 1982; Hatzfeld *et al.* 1997; Davies *et al.* 1997).

STRENGTH OF THE CONTINENTAL CRUST

We have evidence that the strain regime changed within the Aegean since early Quaternary time: (1) microtectonic observations document a change in the direction of extension (e.g. Mercier *et al.* 1979) and (2) some extensional features such as the Gulf of Corinth were reactivated (Armijo *et al.* 1996; Caputo & Pavlides 1993). This change in the tectonics, however, did not create oblique motion on the pre-existing faults bounding the older basins (Karditsa, Larissa, Sporades, Evia) which formed during the Pliocene. In contrast, the creation of new faults striking perpendicular to the orientation of principal extension generally occurred. We observe that the style of faulting is different between Central Greece, whose crust is certainly of continental type (Makris 1978), and the Northern Aegean, whose crust has been stretched by a factor of 2 (Le Pichon & Angelier 1979) and therefore probably thinned. This supports the idea that the strength of thick crust is less than that of thinner crust

If new faults are created in the continental crust of Central Greece, this implies that the work necessary to break the continental crust is smaller than or equal to the work necessary to reactivate old structures that strike obliquely to the direction of extension. Therefore, the reactivation of faults is not a unique process that accommodates the deformation of the continental crust, and old faults behave as zones of weakness only under certain conditions. However, this work is not very much smaller because earthquakes such as the 1894 Atalanti-Martinon event rarely occur on faults that strike obliquely.

The reactivation of a pre-existing fault depends on several parameters such as the values of the principal stresses, their orientations relative to the fault plane, and the friction law (Célérier 1988). It is usually solved graphically on a Mohr diagram (Fig. 15). In the following, we will assume several hypotheses in order to simplify the computation: (1) a fault dip of about 45°, which is roughly the case for a pre-existing normal fault (e.g. Atalanti); (2) a σ_3 principal stress which is horizontal, trending N–S and oriented at 45° to the strike of the pre-existing fault (which is the orientation of most of the pre-existing faults as Pilio and Atalanti); (3) a uniaxial extensional stress field with $\sigma_1 \approx \sigma_2$ (which is likely to be the case for the southern Aegean); (4) an angle of internal friction of $\phi = 30°$ and a negligible cohesion τ_0 (Byerlee 1978). We can therefore estimate roughly the ratio between $\mu_f = \tan \phi_f$ (the friction on the pre-existing fault) and μ_0 (the internal friction for a new fault). If we observe simultaneously earthquakes on

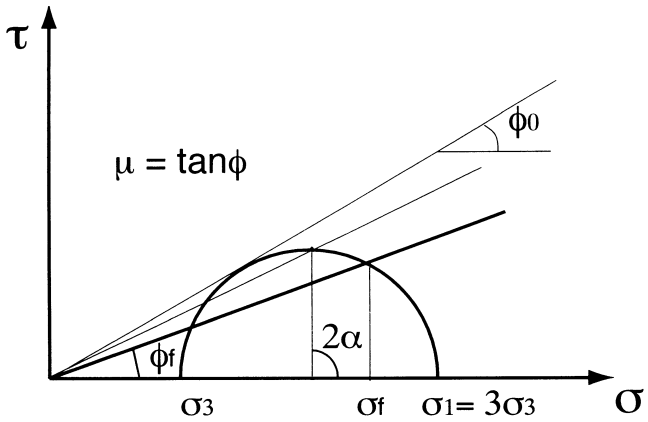

Figure 15. Mohr diagram describing the stress regime between a new fault and a pre-existing fault. The dips of the new fault and the pre-existing fault are 45°. The difference in strike between σ_3 and the new fault is 90° and between σ_3 and the pre-existing fault is 45°. The angle of internal friction $\phi_0 = 30°$ and the cohesion τ_0 is zero. The value of the effective stress on the pre-existing fault is $\sigma_f = 3/4\sigma_1 + 1/4\sigma_3 = 5\sigma_3/2$. The inferred strength of the pre-existing fault is $\mu_f = \tan \phi_f$, which is not very much smaller than $\mu_0 = \tan \phi_0$.

pre-existing faults and earthquakes that create new faults, the ratio μ_f/μ_0 is about 0.70. This ratio increases if the stress field is not uniaxial ($\sigma_1 > \sigma_2 > \sigma_3$). It does not depend very much on the dip of the fault. This means that pre-existing faults are not very much weaker than the flawless crust, and it may be easier in some case to create new faults than to reactivate faults that strike obliquely to the principal stress.

CONCLUSIONS

The microearthquakes that we recorded during seven weeks with a temporary seismological network complement the seismicity picture (both historical and instrumental) that we have for Thessaly and the western termination of the North Aegean Trough. We confirm strike-slip motion along the North Aegean Trough, which has probably been active since Pliocene time. This strike-slip motion is transferred into normal faulting (with the direction of principal extension being constant) in continental Greece. This normal faulting is associated with recent normal faults that are observed around the Gulf of Volos and the Lamia Basin and cut across older important faults which were active during the Miocene, but are oriented obliquely to the direction of extension.

Our data suggest that it is easier to break the continental crust of mainland Greece, perpendicular to the main direction of extension, than to activate obliquely oriented pre-existing faults. This implies that the strength of continental crust is similar to that with pre-existing faults. Where the crust has thinned substantially, however, pre-existing weak zones do localize deformation.

Finally, the scatter in distribution of the slip vectors which are related to the motion of crustal blocks contrasts with the homogenous T-axes pattern.

ACKNOWLEDGMENTS

We thank all the observers who helped us in maintaining the seismological stations: P. Bernard, R. Bossu, M.-P. Bouin,

Y. Breton, G. Chircea, P. Cossec, K. Descours, M. Guillot, M. Hardt, G. Karakaisis, B. Karakostas, G. Karantonis, A. Kiratzi, Y. Klinger, C. Lachet, D. Legrand, S. Lebegat, V. Lignier, T. Merle d'Aubigné, Y. Moreau, F. Nino, E. Papadimitriou, C. Papadopoulos, P. Pinetes, J. Revilla, C. Rodoyannis, T. Tsapanos, P. Triantafyllidis, B. Urgelli, P. Voidomatis and N. Voulgaris, amongst others. We benefited from important support from H. Lyon-Caen, B. Papazachos and J. Drakopoulos and from interesting discussions with J. Jackson and P. Molnar. J. Martinod. P. Molnar, R. Caputo and an anonymous reviewer made constructive criticisms. D. Booth kindly made available to us his data. This work was supported by EEC Contract EPOCH-CT91–0043.

REFERENCES

Ambraseys, N. & Jackson, J., 1990. Seismicity and associated strain of Central Greece between 1890 and 1988, *Geophys. J. Int.,* **101,** 663–708.

Angelier, J., Lyberis, N., Le Pichon, X., Barrier, E. & Huchon, P., 1982. The neotectonic development of the Hellenic Arc and the Sea of Crete: a synthesis, *Tectonophysics,* **86,** 159–196.

Armijo, R., Meyer, B., King, G.C.P., Rigo, A. & Papanastassiou, D., 1996. Quaternary evolution of the Corinth Rift and its implications for the late Cenozoic evolution of the Aegean, *Geophys. J. Int.,* **126,** 11–53.

Billiris, H. *et al.,* 1991. Geodetic determination of the strain of Greece in the interval 1900–88, *Nature,* **350,** 124–129.

Byerlee, J.D., 1978. Friction of rocks, *Pageoph,* **116,** 615–626.

Caputo, R., 1990. Geological and structural study of the Recent and active brittle deformation of the Neogene-Quaternary basins of Thessaly (Central Greece), *Sci. Ann. Geol. Dept,* Spec. Publ. Aristotle University of Thessaloniki, Greece.

Caputo, R., 1995. Inference of a seismic gap from geological data: Thessaly (Central Greece) as a case study, *Ann. Geophys.,* **38,** 1–19.

Caputo, R., 1996. The active Nea Anchialos Fault System (Central Greece): comparison of geological, morphotectonic, archaeological and seismological data, *Ann. Geophys.,* **39,** 557–574.

Caputo, R. & Pavlides, S., 1993. Late Cainozoic geodynamic evolution of Thessaly and surroundings (central-northern Greece), *Tectonophysics,* **223,** 339–362.

Célérier, B., 1988. How much does slip on a reactivated fault plane constrain the stress tensor?, *Tectonics,* **7,** 1257–1278.

Davies, R., England, P., Parsons, B., Billiris, H., Paradissis, D. & Veis, G., 1997. Geodetic strain of Greece in the interval 1892–1992, *J. geophys. Res.,* **102,** 24 571–24 588.

De Mets, C., Gordon, R.G., Argus, D.F. & Stein, S., 1990. Current plate motions, *Geophys. J. Int.,* **101,** 425–478.

Dinter, D.A. & Royden, L., 1993. Late Cenozoic extension in north-eastern Greece: Strymon Valley detachment system and Rhodope metamorphic core complex, *Geology,* **21,** 45–48.

England, P. & Jackson, J., 1989. Active deformation of the continents, *Ann. Rev. Earth. planet. Sci.,* **17,** 197–226.

England, P. & McKenzie, D., 1982. A thin viscous sheet model for continental deformation, *Geophys. J. R. astr. Soc.,* **70,** 295–321.

England, P., Houseman, G. & Sonder, L., 1985. Length scales for continental deformation in convergent, divergent, and strike slip environments: analytical and approximate solutions for a thin viscous sheet model, *J. geophys. Res.,* **90,** 3551–3557.

Hatzfeld, D. & Martin, Ch., 1991. The Aegean intermediate seismicity defined by ISC data, *Earth planet. Sci. Lett.,* **113,** 267–275.

Hatzfeld, D., Christodoulou, A.A., Scordilis, E.M., Panagiotopoulos, D.G. & Hatzidimitriou, P.M., 1987. A microearthquake study of the Mygdonian graben (Northern Greece), *Earth planet. Sci. Lett.,* **81,** 379–396.

Hatzfeld, D., Pedotti, G., Hatzidimitriou, P. & Makropoulos, K., 1990. The strain pattern in the western Hellenic arc deduced from a microearthqauke survey, *Geophys. J. Int.,* **101,** 181–202.

Hatzfeld, D., Kassaras, I., Panagiotopoulos, D., Amorese, D., Makropoulos, K., Karakaisis, G. & Coutant, O., 1995. Microseismicity and strain pattern in Northwestern Greece, *Tectonics,* **14,** 773–785.

Hatzfeld, D., Martinod, J., Bastet, G. & Gautier, P., 1997. An analog model for the Aegean to describe the contribution of gravitational potential energy, *J. geophys. Res.,* **102,** 649–659.

Jackson, J.A., 1994. The Aegean deformation, *Ann. Rev. Earth planet. Sci.,* **22,** 239–272.

Jackson, J. & McKenzie, D., 1984. Rotational mechanisms of active deformation in Greece and Iran, in *The Geological Evolution of the Eastern Mediterranean,* eds Dixon, J.E. & Robertson, A.H.F., *Geol. Soc. Lond. Spec. Publ.,* **17,** 743–754.

Jackson, J.A. & McKenzie, D., 1988. The relationship between plate motions and seismic moment tensors, and the rates of active deformation in the Mediterranean and the Middle East, *Geophys. J.,* **93,** 45–73.

Jolivet, L., Brun, J.-P., Gautier, P., Lallemand, S. & Patriat, M., 1994. 3-D kinematics of extension in the Aegean from early Miocene to the present: insight from ductile crust, *Bull. Soc. géol. Fr.,* **165,** 195–209.

Kastens, K., Gilbert, L.E., Hurts, K., Veis, G., Paradissis, D., Billiris, H., Sclüter, W. & Seeger, H., 1995. GPS evidence for arc-parallel extension along the Hellenic Arc, Greece, *Tectonophysics,* submitted.

Kissel, C., Laj, C. & Mazaud, A., 1986. Paleomagnetic results from Neogene formations in Evia, Skyros, and the Volos region and the deformation of Central Aegea, *Geophys. Res. Lett.,* **13,** 1446–1449.

Lamb, S., 1994. Behavior of the brittle crust in wide plate boundary zones, *J. geophys. Res.,* **99,** 4457–4483.

Lee, W.H.K. & Lahr, J.C., 1972. HYPO71 (revised), a computer program for determining hypocenters, magnitude and first motion pattern of local earthquakes, *USGS Open File Rept,* 75–311.

Lemeille, F., 1977. Etudes néotectoniques en Grèce centrale nord-orientale (Eubée Centrale, Attique, Béotie, Locride) et dans les Sporades du nord (ile de Skiros), Thèse de 3ème cycle de l'Université de Paris XI, France.

Le Pichon. X., 1982. Land-locked oceanic basins and continental collision: the eastern Mediterranean as a case example, in *Mountain Building Processes,* pp. 210–211, ed. Hsü, K.J., Academic Press, New York.

Le Pichon, X. & Angelier, J., 1979. The Hellenic arc and trench system: a key to the neotectonic evolution of the Eastern Mediterranean region, *Tectonophysics,* **60,** 1–42.

Le Pichon, X., Lyberis, N. & Alvarez, F., 1985. Subsidence history of the North Aegean Trough, in *The Geological Evolution of the Eastern Mediterranean,* eds Dixon, J.E. & Robertson, A.H.F., *Geol. Soc. Lond. Spec. Publ.,* **17,** 727–741.

Le Pichon, X., Chamot-Rooke, N., Lallemant, S., Noomen, R. & Veis, G., 1995. Geodetic determination of the kinematics of Central Greece with respect to Europe: implications for Eastern Mediterranean Tectonics, *J. geophys. Res.,* **100,** 12 675–12 690.

Lyberis, N., 1984. Tectonic evolution of the North Aegean Trough, in *The Geological Evolution of the Eastern Mediterranean,* eds Dixon, J.E. & Robertson, A.H.F., *Geol. Soc. Lond. Spec. Publ.,* **17,** 708–725.

Makris, J., 1978. The crust and upper mantle structure of the Aegean region from deep seismic soundings, *Tectonophysics,* **46,** 269–284.

Mascle, J. & Martin, L., 1990. Shallow structure and recent evolution of the Aegean Sea: a synthesis based on continuous reflection profiles, *Mar. Geol.,* **94,** 271–299.

McKenzie, D.P., 1972. Active tectonics of the Mediterranean region, *Geophys. J. R. astr. Soc.,* **30,** 109–185.

McKenzie, D.P., 1978. Active tectonics of the Alpine-Himalayan belt: the Aegean Sea and surrounding regions, *Geophys. J. R. Astr. Soc.,* **55,** 217–254.

McKenzie, D. & Jackson, J., 1983. The relationship between strain rates, crustal thickening, palaeomagnetism, finite strain and fault movements within a deforming zone, *Earth planet. Sci. Lett.,* **65,** 182–202.

Mercier, J.L., Carey, E., Philip, H. & Sorel, D., 1976. La néotectonique plio-quaternaire de l'arc égéen externe et de la mer Egée et ses relations avec la sismicité, *Bull. Soc. géol. Fr.,* **7,** 355–372.

Mercier, J.L., Delibasis, N., Gautier, A., Jarrige, J.J., Lemeille, F., Philip, H., Sébrier, M. & Sorel, D., 1979. La néotectonique de l'Arc Egéen, *Rev. Géol. Dyn. Géogr. Phys.,* **21,** 67–92.

Mercier, J.L., Carey-Gailhardis, E., Mouyaris, N., Simeakis, C., Roudoyanni, T. & Angelidhis, C., 1983. Structural analysis of recent and active faults and regional state in the epicentral area of the 1978 Thessaloniki earthquake (Northern Greece), *Tectonics,* **2,** 577–600.

Mercier, J.L., Sorel, D., Vergely, P. & Simeakis, K., 1989. Extensional tectonic regimes in the Aegean basins during the Cenozoic, *Basin Res.,* **2,** 49–71.

Molnar, P., 1988. Continental tectonics in the aftermath of plate tectonics, *Nature*, **335,** 131–137.

Noomen, R., *et al.,* 1995. Earth rotation and station coordinates computed from SLR and GPS observations: EOP (DUT) 95L02 and SSC (DUT) 95C02, in *Earth Orientation, Reference Frames and Atmospheric Excitation Functions Submitted. for the 1994 IERS Annual Rept,* pp. L13–L20, ed. Charlot, P., *IERS Technical Note,* 19.

Nur, A., Ron, H. & Scotti, O., 1986. Fault mechanics and the kinematics of block rotation, *Geology,* **14,** 746–749.

Papastamatiou, D. & Mouyaris, N., 1986. The earthquake of April 30, 1954, in Sophades (Central Greece), *Geophys. J. R. astr. Soc.,* **87,** 885–895.

Papazachos, B. & Papazachou, K., 1997. The earthquakes of Greece, *Ekdoseis Ziti,* Thessaloniki.

Papazachos, B.C., Panagiotopoulos, D.G., Tsapanos, T.M., Mountrakis, D.M. & Dimopoulos, G.C., 1983. A study of the summer seismic sequence in the Magnesia region of Central Greece, *Geophys. J. R. astr. Soc.,* **75,** 155–168.

Papazachos, C.B. & Kiratzi, A.A., 1996. A detailed study of the active crustal deformation in the Aegean and surrounding area, *Tectonophysics,* **253,** 129–153.

Pavlides, S. & Caputo, R., 1994. The North Aegean region: a tectonic paradox?, *Terra Nova,* **6,** 37–44.

Pavlides, S.B. & Mountrakis, D.M., 1987. Extensional tectonics of northwestern Macedonia, Greece, since the late Miocene, *J. struct. Geol.,* **9,** 385–392.

Pavlides, S.B. & Tranos, M.D., 1991. Structural characteristics of two strong earthquakes in the North Aegean: Ierissos (1932) and Agios Efstratios (1968), *J. struct. Geol.,* **13,** 205–214.

Philip, H., 1976. Un épisode de déformation en compression à la base du Quaternaire en Grèce Centrale (Locride, Grèce), *Bull. Soc. géol. Fr.,* **28,** 287–292.

Robbins, J.W., Torrence, M.H., Dunn, P.J. & Smith, D.E., 1994. Deformation in the Eastern Mediterranean, *1st Turkish Symp. on Deformations,* Istanbul, 5–9 September.

Roberts, S. & Jackson, J.A., 1991. Active normal faulting in Central Greece: and overview, in *The Geometry of Normal Faults,* eds Roberts, A.M., Yielding, G. & Freeman, B., *Geol. Soc. Lond. Spec. Publ.,* **56,** 125–142.

Tapponnier, P., 1977. Evolution tectonique du système alpin en Méditerranée: poinçonnement et écrasement rigide plastique, *Bull. Soc. géol. Fr.,* **3,** 437–460.

Taymaz, T., Jackson, J.A. & McKenzie, D., 1991. Active tectonics of the North and Central Aegean Sea, *Geophys. J. Int.,* **106,** 433–490.

APPENDIX A: LOWER-HEMISPHERE FOCAL MECHANISMS

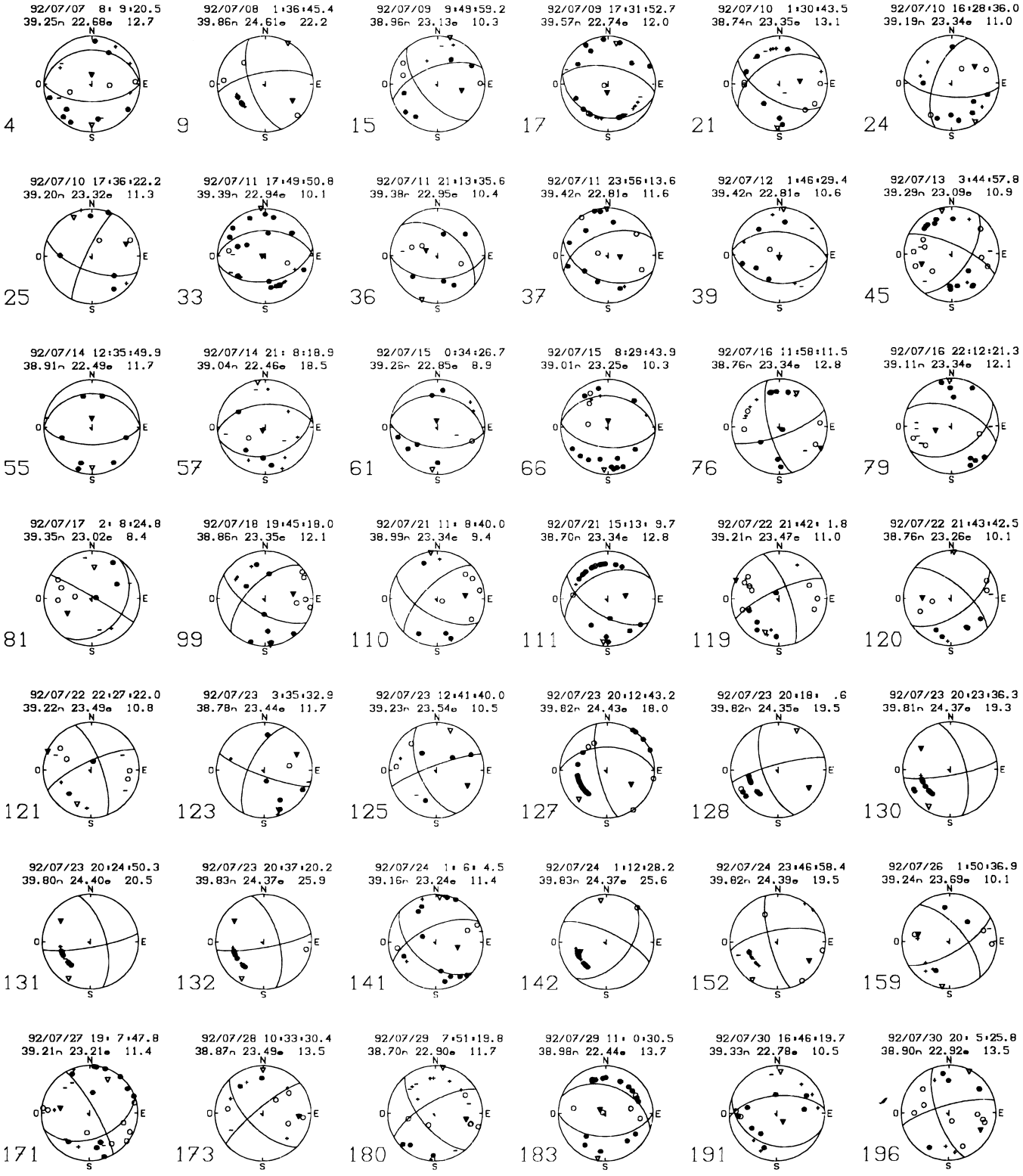

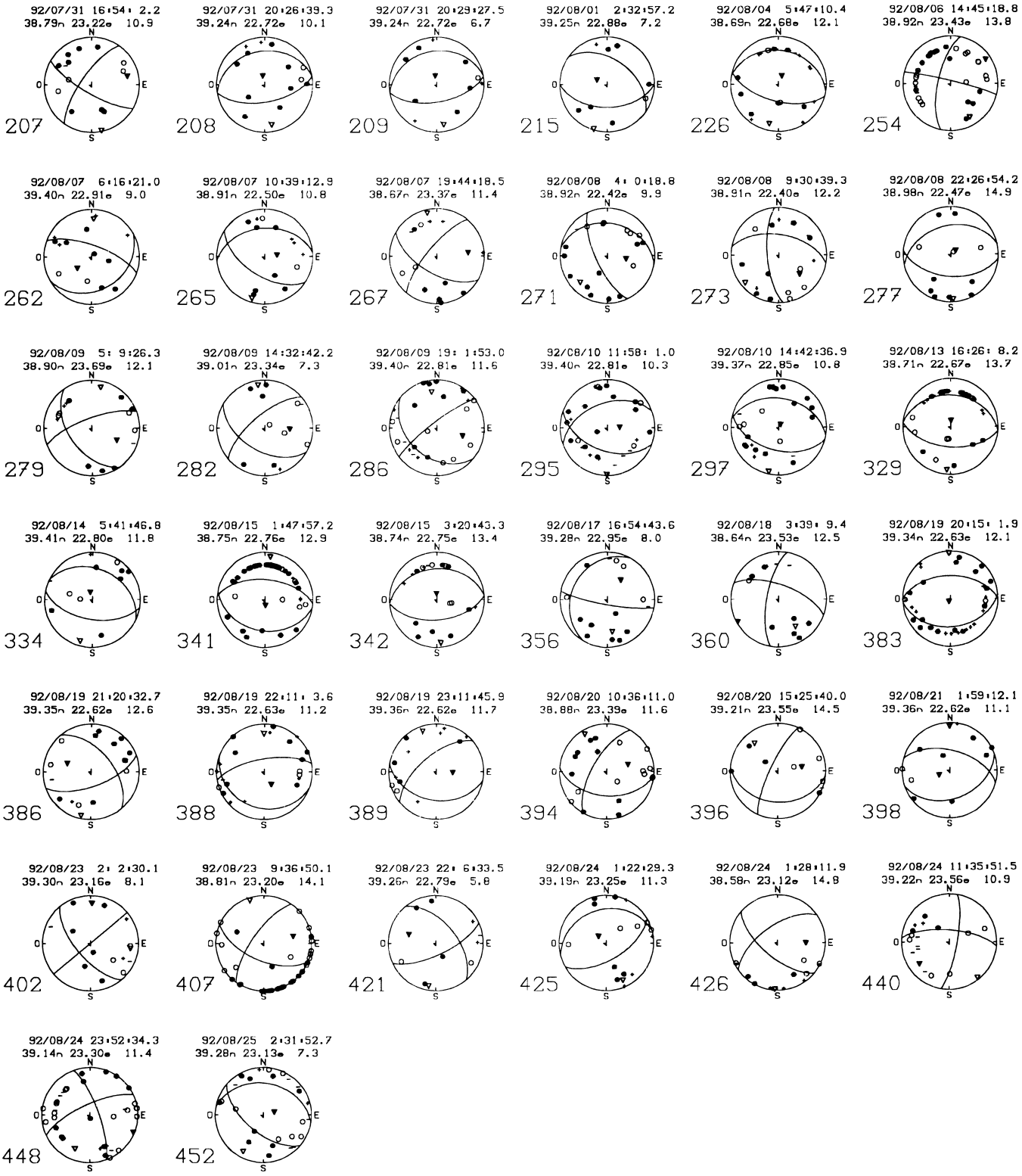
92/07/31 16:54: 2.2
38.79N 23.22E 10.9
207
92/07/31 20:26:39.3
39.24N 22.72E 10.1
208
92/07/31 20:29:27.5
39.24N 22.72E 6.7
209
92/08/01 2:32:57.2
39.25N 22.88E 7.2
215
92/08/04 5:47:10.4
38.69N 22.68E 12.1
226
92/08/06 14:45:18.8
38.92N 23.43E 13.8
254
92/08/07 6:16:21.0
39.40N 22.91E 9.0
262
92/08/07 10:39:12.9
38.91N 22.50E 10.8
265
92/08/07 19:44:18.5
38.67N 23.37E 11.4
267
92/08/08 4: 0:18.8
38.92N 22.42E 9.9
271
92/08/08 9:30:39.3
38.91N 22.40E 12.2
273
92/08/08 22:26:54.2
38.98N 22.47E 14.9
277
92/08/09 5: 9:26.3
38.90N 23.69E 12.1
279
92/08/09 14:32:42.2
39.01N 23.34E 7.3
282
92/08/09 19: 1:53.0
39.40N 22.81E 11.6
286
92/08/10 11:58: 1.0
39.40N 22.81E 10.3
295
92/08/10 14:42:36.9
39.37N 22.85E 10.8
297
92/08/13 16:26: 8.2
39.71N 22.67E 13.7
329
92/08/14 5:41:46.8
39.41N 22.80E 11.8
334
92/08/15 1:47:57.2
38.75N 22.76E 12.9
341
92/08/15 3:20:43.3
38.74N 22.75E 13.4
342
92/08/17 16:54:43.6
39.28N 22.95E 8.0
356
92/08/18 3:39: 9.4
38.64N 23.53E 12.5
360
92/08/19 20:15: 1.9
39.34N 22.63E 12.1
383
92/08/19 21:20:32.7
39.35N 22.62E 12.6
386
92/08/19 22:11: 3.6
39.35N 22.63E 11.2
388
92/08/19 23:11:45.9
39.36N 22.62E 11.7
389
92/08/20 10:36:11.0
38.88N 23.39E 11.6
394
92/08/20 15:25:40.0
39.21N 23.55E 14.5
396
92/08/21 1:59:12.1
39.36N 22.62E 11.1
398
92/08/23 2: 2:30.1
39.30N 23.16E 8.1
402
92/08/23 9:36:50.1
38.81N 23.20E 14.1
407
92/08/23 22: 6:33.5
39.26N 22.79E 5.8
421
92/08/24 1:22:29.3
39.19N 23.25E 11.3
425
92/08/24 1:28:11.9
38.58N 23.12E 14.8
426
92/08/24 11:35:51.5
39.22N 23.56E 10.9
440
92/08/24 23:52:34.3
39.14N 23.30E 11.4
448
92/08/25 2:31:52.7
39.28N 23.13E 7.3
452